CHARLES UNIVERSITY

FACULTY OF PHARMACY IN HRADEC KRALOVÉ

Department of Pharmaceutical Chemistry and Pharmaceutical Analysis

SYNTHESIS OF COUMARIN BASED FLUOROPHORE PROBES

DIPLOMA THESIS

Barbora Koutníková

Supervisor: prof. PharmDr. Martin Doležal, PhD.

Hradec Králové 2023

This work was performed during Erasmus+ stay in:

**University of Ljubljana
Faculty of Pharmacy
Department of Pharmaceutical Chemistry**

Under supervision of:

Prof. Janez Ilaš, M. Pharm., Ph.D.

And revised in:

**Charles University
Faculty of Pharmacy in Hradec Králové
Department of Pharmaceutical Chemistry and Pharmaceutical
Analysis**

Under supervision of:

prof. PharmDr. Martin Doležal, Ph.D.

ACKNOWLEDGEMENT

I would like to express my greatest gratitude to Prof. Janez Ilaš, M. Pharm., Ph.D. for allowing me to work on this project in the Department of Pharmaceutical Chemistry at University of Ljubljana and for supervising me during my Erasmus+ stay in Slovenia. My sincere gratitude also goes to my supervisor prof. PharmDr. Martin Doležal, Ph.D. for kind support during activities related to this project.

A special thanks goes to my consultant MSc. Daria Nawrot, who patiently guided me through my beginnings in the laboratory at the faculty in Hradec Králové, gave me valuable advice any time I needed one, and helped me to put together this thesis and other projects in previous years.

I would like to acknowledge the assistance of Ilaria Brau, M. Pharm., who shared her practical laboratory experiences with me during my Erasmus+ stay, and Mgr. Marek Kerda, who helped me with activities related to this project.

Lastly, I would like to thank all the master's students, PhD students, Assistants, and researchers with whom I shared the laboratory in Ljubljana and who navigated me around and created friendly atmosphere.

Table of Contents

Abstract

Cancer remains to be one of the leading causes of death worldwide. Despite the progress in anti-cancer treatment, therapy of cancer is still associated with many disadvantages including an absence of selectivity as a major issue. The aim in development of chemotherapeutic drugs is to prepare more selective and better tolerated anti-cancer agents.

Topoisomerases play an important role in the therapy of bacterial infections as well as anti-cancer treatment. Both types (human topo I and II) can be targeted during anti-cancer therapy. Isoform IIα is overexpressed during proliferation of the cell and therefore it is characteristic for cancer cells. Inhibition of this isoform leads to excessive DNA damage or to malfunctions during cell proliferation and consequently to cell apoptosis. This is why inhibitors of topoisomerase IIα are studied as candidates for anti-cancer therapy.

The aim of this work was to prepare three compounds that would be later tested for inhibitory activity on human topoisomerase IIα. Optimization of the reaction conditions was performed during the synthesis and successfully obtained compound was purified to allow further *in vitro* testing. Results of the testing and details regarding the synthetic procedures will be discussed in the thesis.

Abstrakt

Rakovina se celosvětově řadí mezi hlavní příčiny úmrtí. I přes neustálý rozvoj na poli léčby rakoviny tato terapie zůstává spojena s mnoha problémy, mezi něž se řadí i absence selektivity užívaných léčivých látek. Cílem vývoje chemoterapeutických látek je proto snaha připravit selektivnější a lépe tolerované sloučeniny.

Topoizomerázy hrají důležitou roli v terapii bakteriálních infekcí a také v terapii rakoviny. Na oba typy tohoto enzymu (lidská topoizomeráza I i II) je možné při léčbě rakoviny cílit. Izoforma IIα je exprimována ve velkém množství v proliferujících buňkách a její výskyt je tedy typický právě pro rakovinné buňky. Inhibice této izoformy vede k významnému poškození DNA nebo k poruchám v průběhu dělení buněk a následně může vést k buněčné apoptóze. Tyto mechanismy dělají z inhibitorů topoizomerázy IIα potenciální kandidáty pro léčbu rakoviny.

Cílem práce bylo připravit tři sloučeniny a následně otestovat jejich inhibiční aktivitu na lidské topoizomeráze IIα. Reakční podmínky některých kroků syntézy byly v průběhu přípravy sloučenin optimalizovány a získaná sloučenina byla následně purifikována pro testování *in vitro*. Výsledky testování a podrobnosti týkající se přípravy jednotlivých sloučenin budou popsány v rámci této práce.

Abbreviations

ATP – adenosine triphosphate

(Boc)$_2$O – di-*tert*-butyl dicarbonate

BODIPY – Dipyrrometheneboron difluoride

DCM – dichloromethane

DIPEA – *N,N*-Diisopropylethylamine

DMF – *N,N*-Dimethylformamide

DMS – dimethyl sulfate

EGCG – epigallocatechin gallate

EtOH – ethanol

FRET system – fluorescence resonance energy transfer system

HEPES buffer – *N*-2-hydroxyethylpiperazine-*N*-2-ethane sulfonic acid buffer

HepG2 – human liver cancer cell line

^{1}H NMR – proton nuclear magnetic resonance

HPLC-MS – high-performance liquid chromatography-mass spectrometry

hTopoI – human topoisomerase I

hTopoIIα – human topoisomerase IIα

IC$_{50}$ – half-maximal inhibitory concentration

MCF-7 – breast cancer cell line

MeOH – methanol

NIR – near-infrared region

RT – room temperature

TEA – triethylamine

THF – tetrahydrofuran

TLC – thin-layer chromatography

topo I – topoisomerase I

topo II – topoisomerase II

topo IIα – topoisomerase IIα

topo IIβ – topoisomerase IIβ

UV – ultraviolet

WHO – World Health Organization

Aim of work

The aim of this work was to prepare three compounds and subsequently evaluate their inhibitory activity on hTopoIIα. Two of these compounds share similar structural pattern with agents previously synthetized at the University of Ljubljana.[1] These two compounds with fluorophore incorporated in their structure in position 2 of the benzene ring (Fig. 1) would be later used to observe distribution of the compounds and interactions with various components of cells using fluorescence cell microscopy.
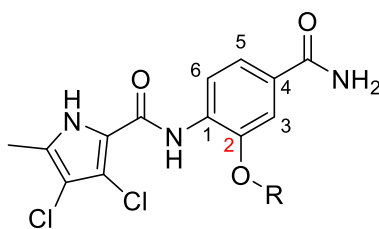
Fig. 1 General structure of two intended compounds.

The third compound (Fig. 2) is structurally distinct from previously prepared agents. However, it is believed to have potential to exhibit inhibitory activity on hTopoIIα.
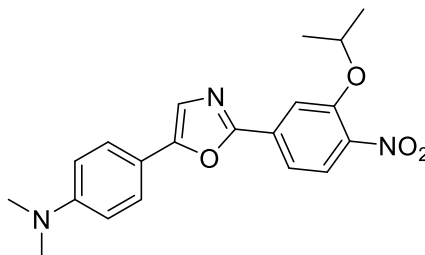
Fig. 2 IBK-11.

1. Introduction

According to International Agency for Research on Cancer (forming part of WHO) cancer is one of the leading causes of death. In 2020 it caused nearly 10 million deaths worldwide.[2] Even though there are anti-cancer drugs approved for use in clinical practice, finding new chemotherapeutic substances is still important due to disadvantages associated with current anti-cancer treatment. Poor selectivity, often resulting in severe side effects (e.g., secondary malignancies, cardiotoxicity, anemia, nausea and dyspepsia, hair loss, edemas), together with development of resistance are major issues that accompany anticancer therapy nowadays.[3] The aim is to develop new entities with improved pharmacokinetic profile, better selectivity and as a result better compliance in patients.

Many structural classes of chemicals are already established as anti-cancer agents (i.e., antimetabolites – antifolates, purine and pyrimidine analogs; anthracyclines; epipodophyllotoxins; camptothecins; platinum analogs; monoclonal antibodies).[4] In this thesis I present a novel compound that belongs to the *N*-Phenylpyrrolamide class and is combined with coumarin scaffold in its structure.

2. Theoretical part

2.1 DNA topoisomerases

DNA topoisomerases are essential enzymes that can be found in both procaryotic and eucaryotic cells. These enzymes are fundamental for processes, such as replication and transcription, that require accessing the information stored in DNA and therefore altering the topological state of DNA strands. Unwinding DNA during these processes leads to undesired helical tension due to double helical structure of DNA. Topoisomerases enable to prevent this topological problem by creating transient single-stranded (topoisomerases type I) or double-stranded (topoisomerases type II) cleavage in DNA molecule that allows to release tension in the double helix.[1,5,6]

Considering that DNA topoisomerases create breaks in DNA double helix makes them dual persona enzymes – on one hand their function is essential for viability of cells but on the other hand they can act as cellular toxins. In a normal state, topoisomerase-DNA cleavage complexes are transient, reversible and enable to perform vital cellular functions. However, if the concentration of cleavage complexes drops low, chromosomes are unable to separate during replication phase and cells die of mitotic failure. On the contrary, if the concentration of cleavage complexes rises to critical levels, excessive damage of the genome overwhelms the cell and initiates apoptotic pathways. This mechanism of action is typical for topoisomerase poisons. Chemotherapeutic agents, such as etoposide and doxorubicin, but even naturally occurring compounds (e.g., bioflavonoid genistein or polyphenol EGCG) which are consumed in human diet, have the ability to increase levels of cleavage complexes and this way convert the enzyme into cellular toxin. Due to their potentially lethal effects, topoisomerases have become a notable target for the development of anti-cancer and antibacterial agents. Human topoisomerase I and human topoisomerase IIα are targeted during anti-cancer therapy, whereas during antibacterial therapy bacterial topoisomerase IV and bacterial gyrase are used as targets.[6–8]

DNA topoisomerases can be divided into two main classes – type I and type II – based on their mechanism of action. Human topoisomerase IIα was used as a target for testing activity of the newly prepared coumarin based compound, therefore information about type II topoisomerases will be discussed in greater detail.

2.1.1 Type I DNA topoisomerases

Type I DNA topoisomerases have monomeric structure and act by creating a transient single-stranded cleavage in the DNA molecule.[5,6]

Bacteria can synthetize three different type I topoisomerases belonging into two subclasses (Table 1). First two enzymes, topoisomerase I and topoisomerase III, belong to type IA subclass. These two enzymes require divalent metal ion (Mg^{2+}) as a cofactor for their catalytic activity. They act by attaching their tyrosine from the active site to the 5′-terminal phosphate of the broken DNA strand. The third topoisomerase that can be produced by bacteria, topoisomerase IB, acts by forming a bond between its tyrosine from the active site and 3′-terminal phosphate of the DNA. Unlike foregoing enzymes, topoisomerase IB does not require Mg^{2+} ions to be functional.[9–11]

Eukaryotes can synthetize two different type I topoisomerases. Topoisomerase I, which is distinct from the bacterial topoisomerase I and belongs to type IB subclass, and topoisomerase III from subclass IA. Inhibitors of human topoisomerase I are used as anticancer agents.[9]

Subclass	Examples	Specifics
IA	Bacterial DNA topoisomerase I Bacterial DNA topoisomerase III Human DNA topoisomerase III (α and β)	Requires divalent metal ion (Mg^{2+}). Bond between the 5′-end of the DNA strand and the catalytic tyrosine. Relaxes only negative supercoils.
IB	Bacterial DNA topoisomerase IB Human DNA topoisomerase I	Does not require divalent metal ion (Mg^{2+}). Bond between the 3′-end of the DNA strand and the catalytic tyrosine. Relaxes both negative and positive supercoils.

Table 1 Occurrence of different subclasses of type I topoisomerases in humans and bacteria (table includes topoisomerases mentioned in this chapter).

2.1.2 Type II DNA topoisomerases

Type II DNA topoisomerases are multimeric enzymes that act by creating a transient double-stranded cleavage in the DNA. Prokaryotic enzymes have heterodimeric structure, eukaryotic enzymes are homodimers. For their activity they require Mg^{2+} ions and energy gained from ATP hydrolysis. To regulate the topology of DNA molecule, two tyrosines from the active-site of the enzyme are bound to two 5′-phosphates in DNA to create a double-stranded cleavage.[5,6,9]
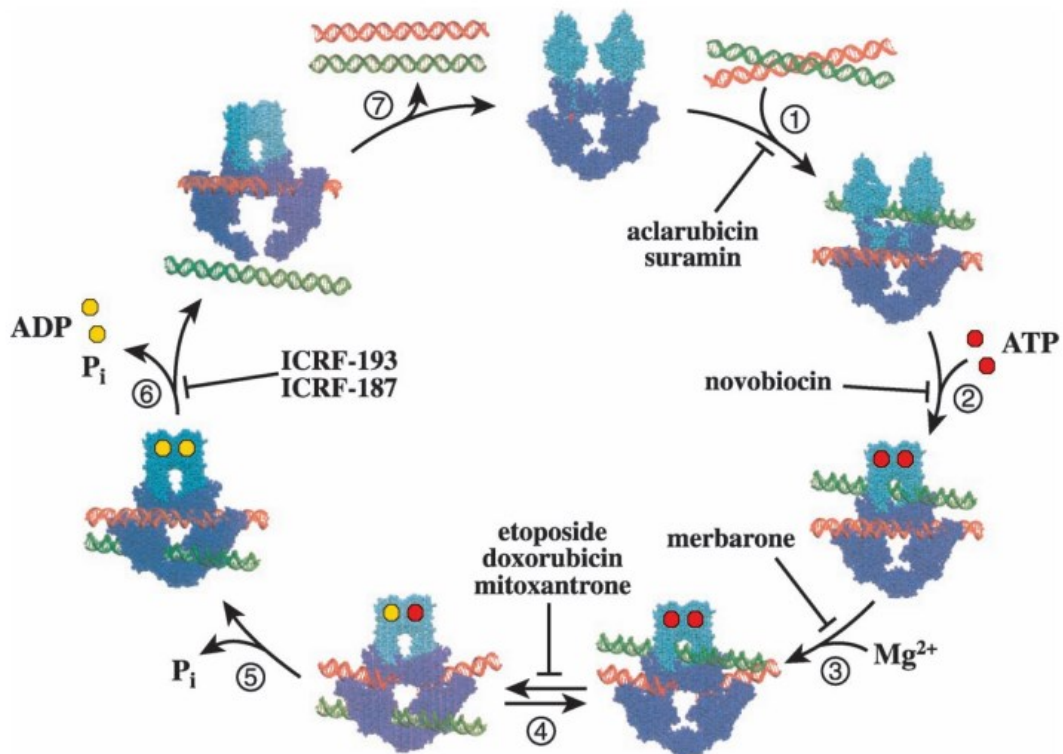
Fig. 3. The catalytic cycle of DNA topoisomerase II. Taken from Larsen et al.[12]

Detailed mechanism of action of DNA topoisomerase II is portrayed in Fig. 3. The catalytic cycle begins with enzyme binding to two double-stranded DNA segments called G segment (gated) and T segment (transported) (step 1). Then, two ATP molecules bind to ATPase domains of the enzyme which leads to dimerization of the two domains (step 2). Mg^{2+} ions are recruited, G segment is cleaved (step 3) and T segment is transported through the originated break, which is facilitated by hydrolysis of one ATP molecule (step 4). The G segment is then reconnected, and second ATP molecule is hydrolyzed (step 5). Next, two ADP molecules are discharged, and the two DNA segments are one by one released (step 6 and step 7).[5,12]

Bacteria encode two different type II enzymes – gyrase and topoisomerase IV. Both are used as targets for antibacterial therapy. Drugs targeting these two enzymes are for example fluoroquinolones (e.g., ciprofloxacin) or aminocoumarin antibiotic novobiocin.[6]

Eukaryotes can synthetize type II enzyme topoisomerase II. Higher eukaryotes express two isoforms of this enzyme – topoisomerase IIα and topoisomerase IIβ. Isoform IIα is overexpressed in proliferating cells where it plays a very important role in replication and in segregating chromosomes during mitosis, which makes isoform IIα a valuable target for anticancer therapy. Topoisomerase IIβ is to be found in cells independently on the cell cycle, but it is expressed widely in cells in post mitotic state. Isoform IIβ does not seem to be crucial for proliferation of the cell, and even though its *in vivo* role is not very well understood, it is apparently associated with everyday processes in cells including reparation of DNA and transcription. It is suggested that isoform IIβ could play a role in toxic effects of topo II poisons, such as secondary malignancies and cardiotoxicity.[13-15]

2.2 DNA topoisomerase inhibitors

As already mentioned, topoisomerases play crucial role in processes including replication, transcription, and chromosome segregation during mitosis. Their function is essential for proliferation and survival of cells therefore inhibition of these enzymes leads to cell death. This fact can be used for therapeutical purposes in both antibacterial and anticancer therapy.

2.2.1 Topo I inhibitors in anticancer therapy

Camptothecin (Fig. 4), natural alkaloid isolated from bark of *Camptotheca accuminata*, was studied for its inhibitory activity on hTopoI, however it shows poor water solubility, low stability in physiological conditions and unpredictable drug-drug interactions. Semi-synthetic derivatives of camptothecin, irinotecan (Fig. 6) and topotecan (Fig. 5), were developed to overcome these obstacles and are now used in clinical practice, even though the chemical instability remains to be an issue.[16,17] Derivatives with optimized properties are being slowly introduced around the world for use in clinical practice. Belotecan, an analog with improved water solubility, was approved by Korean Food and Drug Administration in 2003 for treatment of ovarian and small lung cancer.[18,19] In 2019, U.S. Food and Drug Administration granted an approval to fam-trastuzumab deruxtecan-nxki, an antibody-drug conjugate composed of a monoclonal anti-HER2

antibody linked to exatecan derivative, a topoisomerase I inhibitor. This entity was approved for treatment of unresectable or metastatic HER2-positive breast cancer.[20,21]
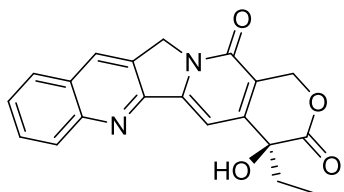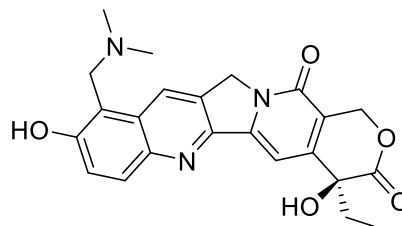

Fig. 4 Chemical structure of camptothecin.

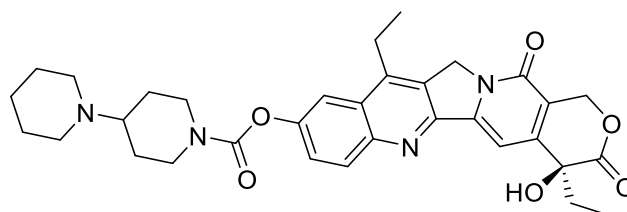*Fig. 5 Chemical structure of topotecan.*

Fig. 6 Chemical structure of irinotecan.

To overcome the instability of camptothecins, structurally distinct non-camptothecin hTopoI inhibitors are investigated, including indolocarbazoles, indenoisoquinolines and dibenzonaphthyridinones. All the above-mentioned compounds act as hTopoI poisons. By turning temporary enzyme-DNA complexes into persistent cytotoxic adducts they cause an excessive DNA damage which eventually leads to cell death.[9]

2.2.2 Topo II inhibitors in anticancer therapy

Topo II inhibitors presently used in anti-cancer therapy are non-specific inhibitors – they inhibit both isoform IIα and IIβ. Inhibition of IIβ isoform is suggested to be associated with severe side effects, therefore one of the aims in development of anti-cancer agents nowadays is to discover selective inhibitors of topoisomerase IIα. Agents selective to IIα isoform have potential to exhibit improved clinical safety compared to non-specific inhibitors.[7,22]

2.2.2.1 Topo II poisons

Despite their toxicity, compounds from this group are used in clinical practice. They act by stabilizing the covalent complex between enzyme and DNA molecule (Fig. 3, step 4). Formation of long-lasting drug-topo II-DNA complexes leads to excessive DNA damage in cells and consequently to cell apoptosis.[13,23] However, if the cell survives the excessive damage, increased levels of cleaved DNA strands in the cell can result in chromosome

10

translocations that can provoke one of the serious side effects occurring when topo II poisons are used in therapy – development of secondary malignancies.[23] Studies show relation between therapeutic use of topo II poisons, such as doxorubicin (Fig. 7) and etoposide (Fig. 8), and development of acute leukemias caused by chromosomal rearrangements.[15,24] Another severe side effect that is related to using topo II poisons, such as doxorubicin and mitoxantrone (Fig. 9), is cardiotoxicity. Even though for a long time the reason for cardiotoxic effect of anthracycline drugs was believed to be production of reactive oxygen species, research showed that the mechanism behind cardiotoxicity is most likely stabilization of topoisomerase isoform IIβ–DNA complexes, which leads to excessive DNA damage in heart, where isoform IIβ appears to be highly expressed.[25,26]
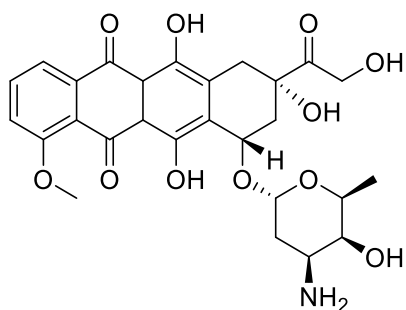
Fig. 7 Chemical structure of doxorubicin.
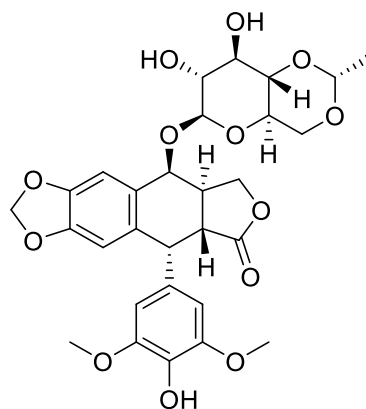
Fig. 8 Chemical structure of etoposide.

Fig. 9 Chemical structure of mitoxantrone.

2.2.2.2 Catalytic inhibitors

Unlike topo II poisons, catalytic inhibitors regulate catalytic activity of topoisomerase II without stabilizing the cleavage complexes. In consequence they do not increase DNA damage in cells and thus have potential to exert lower toxicity compared to topo II poisons. Catalytic inhibitors generally obstruct a step in a catalytic cycle (Fig. 3)

of topoisomerase II that precedes DNA strand cleaving which leads to blockade of essential enzymatic function.[1,8,27]

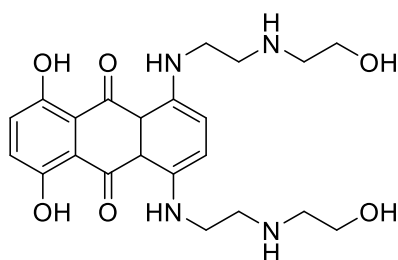There are several mechanisms of action (Table 2) by which catalytic inhibitors can operate. Some of the compounds act by preventing binding of the enzyme to DNA molecule (aclarubicin, suramin).[12,13] ATP-competitive inhibitors (Fig. 3, step 2), which block the ATP binding site of the enzyme, are considered to be the most promising group of catalytic inhibitors.[1,13] Several structural types of ATP-competitive inhibitors have been reported including for example purine analogues, xanthones and thiosemicarbazones.[28] A novel chemotype of ATP-competitive inhibitors, *N*-Phenylpyrrolamides, was discovered at the Faculty of Pharmacy in University of Ljubljana through screening of previously prepared DNA gyrase and topoisomerase IV inhibitors.[13] Newly prepared coumarin based compound IBK-12 described in this thesis is believed to have potential to bind to ATP binding site of human topoisomerase IIα and to act as an inhibitor of this enzyme. Another group including merbarone inhibits cleaving of DNA strands (Fig. 3, step 3).[12] Already mentioned substance, dexrazoxane (also known as ICRF-187), is currently the only catalytic inhibitor used in clinical practice and it is used to prevent the cardiotoxic effect of anthracycline drugs.[25,26] Dexrazoxane possess a dual mechanism of action – binding of dexrazoxane to DNA-topo IIβ complex and fixing it in a closed-clamped conformation around DNA molecule is indicated in Fig. 3 (step 6). Proteasomal degradation of topo IIβ is triggered by this mechanism resulting in down-regulation of topo IIβ. Depletion of this isoenzyme lowers the amount of anthracycline drug that can bind to the enzyme and create DNA-damaging complex.[25]

Mechanism of action	Name of a compound
Preventing binding of the enzyme to DNA	Aclarubicin, suramin
Blockade of ATP-binding site of the enzyme	Novobiocin, *N*-Phenylpyrrolamides
Inhibition of DNA cleaving	Merbarone
Trapping the enzyme in closed-clamp conformation	Dexrazoxane (ICRF-187)

Table 2 Topoisomerase II catalytic inhibitors – mechanisms of action.

2.3 Fluorescence

Fluorescence is a phenomenon characterized by the ability of substance to emit electromagnetic radiation (usually visible light) after previous absorption of electromagnetic radiation of specific wavelengths. Compounds with fluorescent properties usually possess conjugated system of double bonds incorporated in their structure. For the emitted light it is specific that it has longer wavelength than the absorbed light. This fact can be explained with help of Jablonski energy diagram (Fig. 10). After absorption of a photon, an electron is excited from the singlet electronic ground state (S_0) to the singlet electronic excited state (S_1). This process is followed by non-radiative transition within the singlet electronic excited state. During this transition, no photon is emitted, and the energy is released in a form of vibrations or heat. The following fluorescence process characterized by emission of a photon is represented with a green arrow. The fact that fluorescence, unlike absorption, occurs from the lowest vibrational level of the excited state (S_1) to higher vibrational levels of the ground state (S_0) explains why the emitted photon has lower energy (longer wavelength) that the absorbed photon.[29]
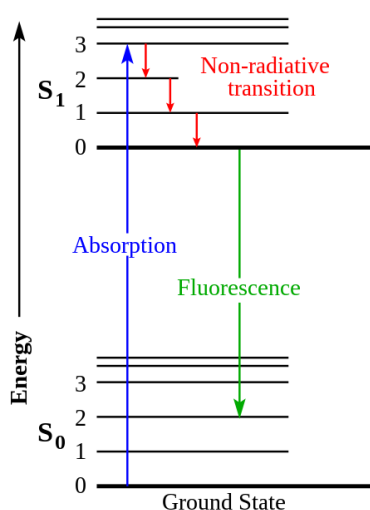
Fig. 10 Jablonski energy diagram. Taken from Kabir et al.[29]
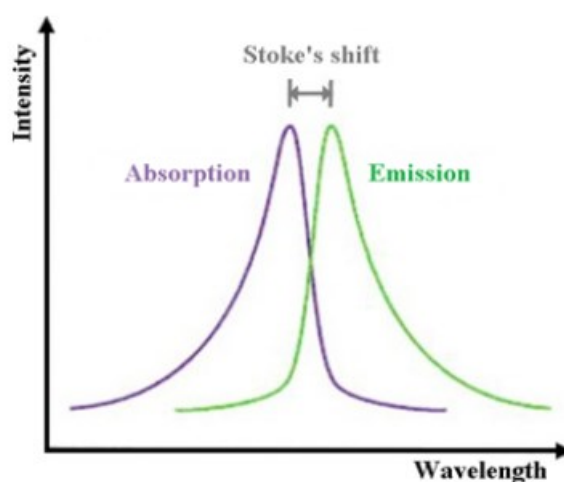
Fig. 11 Stoke's shift. Taken from Kabir et al.[29]

Maximum absorption wavelength and maximum emission wavelength are properties which can be used to describe fluorescent compounds. The difference between these two maximums is called Stoke's shift (Fig. 11). Another important parameters used to characterize fluorophores are quantum yield (number of emitted photons per absorbed photons) and fluorescence life time (time period that the electron spends in the excited state before returning to the ground state).[29]

Not only molecular structure affects fluorescence of given substance. Chemical environment, such as pH level or physicochemical properties of used solvent, have also significant impact on determining intensity and color of emitted light.[29,30]

2.3.1 Coumarin-based fluorophore probes

Coumarins are molecules with sweet odor that occur naturally in a wide variety of plants and contain 2*H*-chromen-2-one motif which introduces conjugated system of double bonds into their structure. In everyday life, coumarins can be found for example in cosmetics, essential oils, or perfumes. In pharmaceutical industry, coumarin scaffold earned a lot of attention due to its exceptional potential in drug design. Broad spectrum of biological effects was described in coumarin-based compounds including anticoagulant activity (e.g., warfarin), antimicrobial activity (e.g., novobiocin) and furthermore anti-neurodegenerative disease, anti-inflammatory and anticancer activities.[31,32]

As a consequence of possessing conjugated system of double bonds in their structure, entities containing coumarin moiety can be additionally used as fluorescent probes with many possible applications. These probes can be utilized as fluorescent chemosensors for anions (e.g., CN^-, F^-) or metal ions (e.g., Cu^+, Cu^{2+}, Hg^{2+}, Fe^{3+}) – for example to detect toxic Hg^{2+} ions in water sources. Heavy metal pollution is a major environmental concern which can negatively affect human health. Therefore, many techniques for effective detection of ions in the environment have been developed, one of them being utilization of coumarin-based compounds as chemosensors. For an illustration, Wu et al. prepared a "turn-on" fluorescent probe with coumarin core and vinyl ether group as a reaction unit (Fig. 12). The probe exhibits no fluorescence in HEPES buffer solution. After reaction with Hg^{2+} ion in a sample, the probe undergoes hydrolysis resulting with 7-hydroxy-4-methylcoumarin as a product of the reaction. This product exhibits strong blue fluorescence with emission maximum at 450 nm.[30–33]
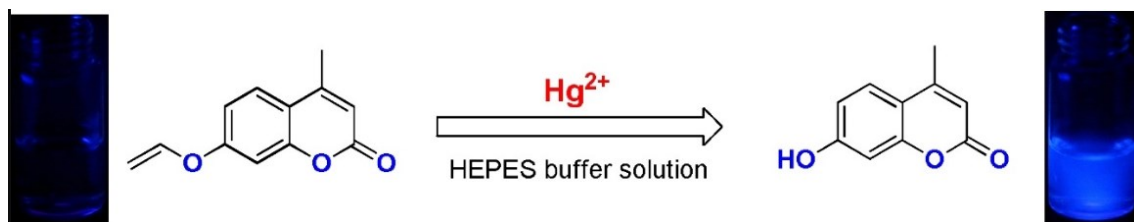

Fig. 12 Fluorescent probe exhibits little to no fluorescence in HEPES buffer solution. On the contrary, product of Hg^{2+}-promoted hydrolysis shows strong blue fluorescence. Taken from Wu et al. [33]

Coumarin fluorescent probes can be as well used as chemosensors for pH levels – for example to detect changes in intracellular pH that can indicate pathological processes such as tumorigenesis or inflammation.[30,32] For an illustration, Zhang et al. developed a coumarin-rhodamine based FRET system as a pH probe (Fig. 13). This system responds to even minor changes in pH range of 4.20–6.00. Spirolactam form of rhodamine does not display fluorescence emission in basic and neutral pH conditions. Addition of H^+ in acidic conditions leads to opening of the lactam ring followed by emission at 582 nm. Therefore, at basic and neutral conditions, only a coumarin blue emission (477 nm) can be detected. In acidic conditions, after the lactam ring is opened, rhodamine becomes an efficient energy acceptor and emits visible light at 582 nm (Fig. 14).[34]
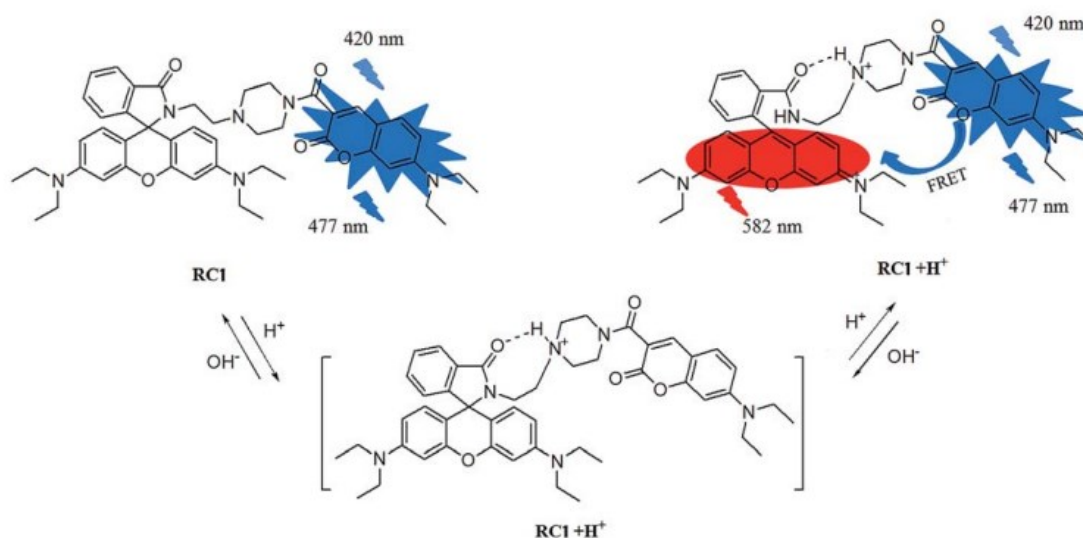

Fig. 13 Lactam ring opening resulting in emission at 582 nm. Taken from Zhang et al.[34]
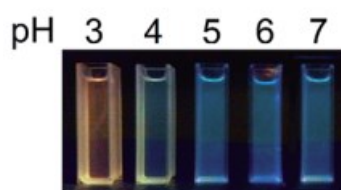

Fig. 14 Visible pH-mediated color changes in a sample treated with a coumarin-rhodamine based FRET system. Taken from Zhang et al.[34]

Coumarin-based fluorophores can be also used as probes for biological imaging. In most cases the coumarin, as a fluorescent part of the molecule, is attached to a recognition unit which is responsible for the reactivity or selectivity. The recognition unit is important for targeting various components of cell, whereas the fluorescent part of the molecule is

important for detection. This way we can target specific parts of cells, observe distribution of the compound in cells or organisms, and analyze binding interactions of the molecule with proteins, DNA, lipids, or membranes.[29,32]

Several problems remain to be limiting for utilization of coumarin-based fluorophores. One of them being poor water solubility of many coumarin-based probes. In aqueous solution, coumarins have tendency to aggregate due to non-covalent π-π interactions which negatively affect solubility in water. Another problem that needs to be resolved relates to the fact that for bioimaging *in vivo* it is favorable, when the compound has ability to be excited and to emit light in the red and NIR region, because electromagnetic radiation of longer wavelengths can pass to deeper layers of the subcutaneous tissue (Fig. 15). Coumarin is a short-wavelength probe meaning it emits usually in the blue region. For *in vivo* use, the coumarin scaffold should be altered to allow absorption and emission in the red or NIR region.[32,35]
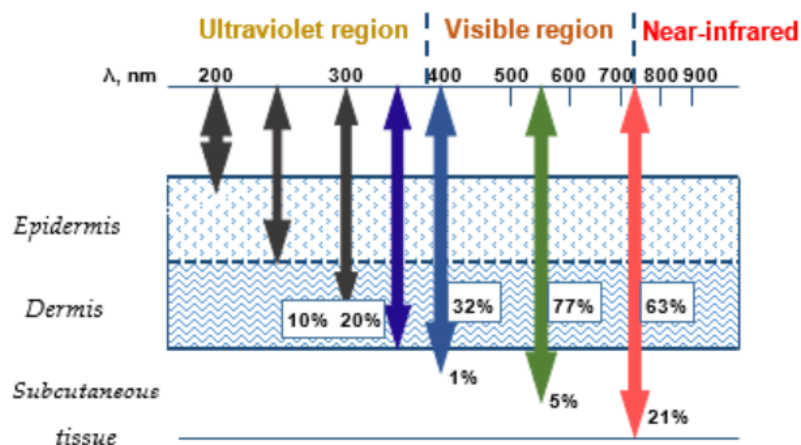

Fig. 15 Permeability of electromagnetic radiation through skin layers to subcutaneous tissue according to wavelength. Taken from Antina et al.[35]

2.4 Structure-activity relationship of *N*-phenylpyrrolamides

N-Phenylpyrrolamides, a novel chemotype of ATP-competitive topo IIα inhibitors, were discovered at the Faculty of Pharmacy in University of Ljubljana through screening of previously prepared DNA gyrase and topoisomerase IV inhibitors. Structure of studied compounds is based on natural entities – oroidin and kibdelomycin (Fig. 16).[13] Oroidin is a marine alkaloid which exhibits antibacterial activity, specifically against Gram-positive bacteria, and kibdelomycin is a natural broad spectrum Gram-positive antibiotic originally isolated from bacterial genus *Kibdelosporangium* sp. which acts by inhibition of bacterial gyrase B and topoisomerase IV.[36,37]
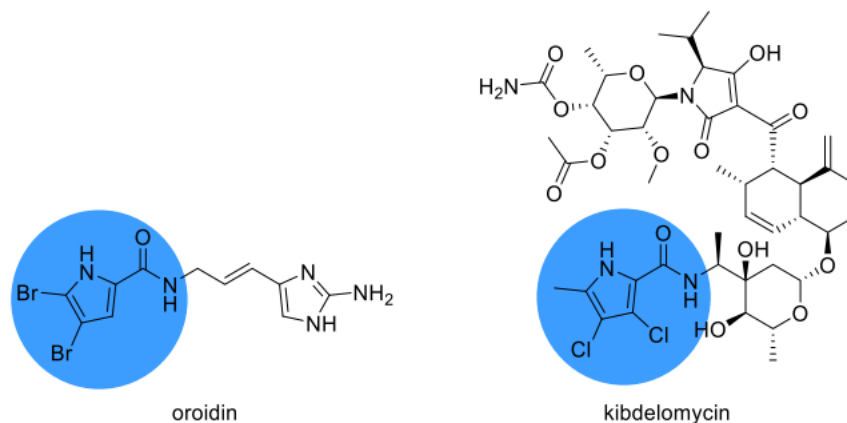
Fig. 16 Structures of oroidin and kibdelomycin with highlighted pyrrolamide moieties. Taken from Žiga et al.[13]
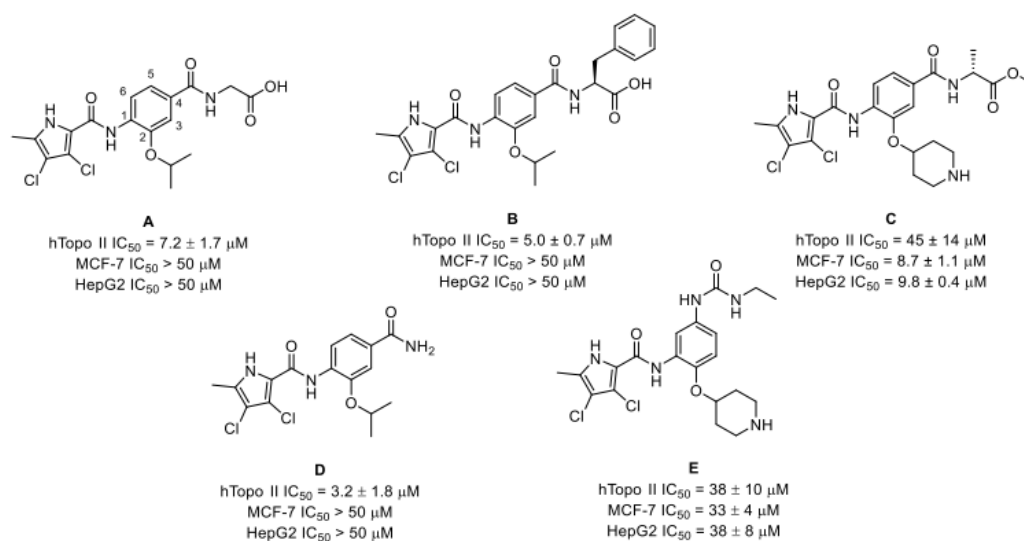

Fig. 17 Structures and activities of main hits from earlier work of researchers from the Faculty of Pharmacy in University of Ljubljana. Taken from Žiga et al.[1]

Compound D (Fig. 17) from the previous work was used as a structural template for further optimization of ATP-competitive topo IIα inhibitors considering that it has low molecular weight and potent activity on the target. The halogen-substituted pyrrole moiety highlighted in Fig. 16 is suggested to be essential for the topo II inhibitory activity. Substances with 3,4-dichloro-5-methylpyrrole moiety in the structure exhibited stronger activities compared to compounds with 4,5-dibromopyrrole, because according to docking results, hydrophobic pocket of the adenine binding site seems to be better suited for dichloromethylpyrrole. The pyrrolecarboxamide moiety is presumed to form two hydrogen bonds with Asn120 and a conserved water molecule. Benzene proved to be effective as a central scaffold with substituents in positions two and four or two and five to maintain the inhibitory activity. Substituents in these positions make a binding mode

of *N*-Phenylpyrrolamides unique since they occupy different binding pockets compared to up to present day known inhibitors. The primary carboxamide group in position four is predicted to form hydrogen bond with Asn150. This amide group is beneficial for the on-target activity. However, the inhibitory activity can be partially preserved with optimal selection of substituent in position two if the group in position four is absent (substituents containing basic group seem to be beneficial for retaining the activity). Despite being advantageous for the on-target activity, amide group in position four is associated with decreased cytotoxicity of prepared compounds. Absence of this primary amide group led to increase in the cytotoxic effects, most likely because of lower polar surface area of prepared compounds, which ensures better passive diffusion into cells. Furthermore, introducing basic centers into the structure through substituent in position two led to increase of cytotoxic effects of the inhibitors. Compound 53b (Fig. 19) shows the most significant cytotoxic effects out of all compounds from the previous research (HepG2 IC_{50} = 130 nM, MCF-7 IC_{50} = 140 nM).[1] Isopropoxy group from the compound D (Fig. 17) was in later studies with advantage replaced by a *para*-substituted or *meta*-substituted *O*-benzyl group. Extending benzyloxy group in position two enables the compound to reach the phosphate-binding region of the ATP binding site and to interact with amino acid residues in this region. Compound 47d (Fig. 18) with ethylenediamine based substituent on the benzyloxy group was the most potent (IC_{50}= 0.67 μM) agent among all inhibitors from the latest study.[1] For better orientation, structure-activity relationship was depicted in Fig. 20.[1,13]
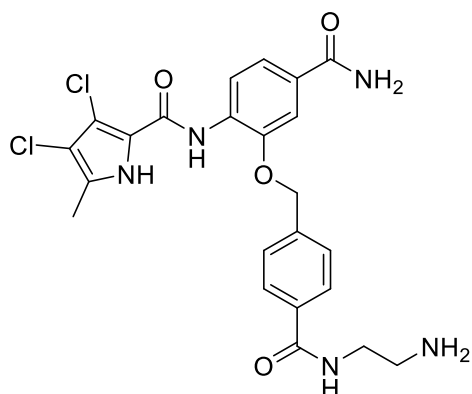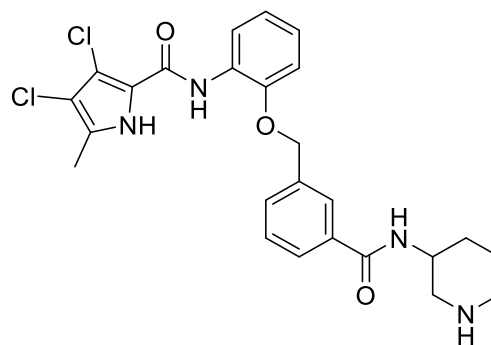

Fig. 18 Compound 47d.

Fig. 19 Compound 53b.

Benzene = central scaffold with substituents in position 2, and position 4 or 5.

Primary amide group is beneficial for the on-target activity.

If missing, activity can be partially retained by the selection of optimal substituent in position 2.

Associated with decreased cytotoxicity.

3,4-dichloro-5-methylpyrrole moiety is essential for the on-target activity.

Para-substituted or *meta*-substituted *O*-benzyl group allows extension of substituent in position 2 – interaction with amino acid residues in phosphate-binding region.

Introduction of basic centers in position 2 leads to increased cytotoxicity.

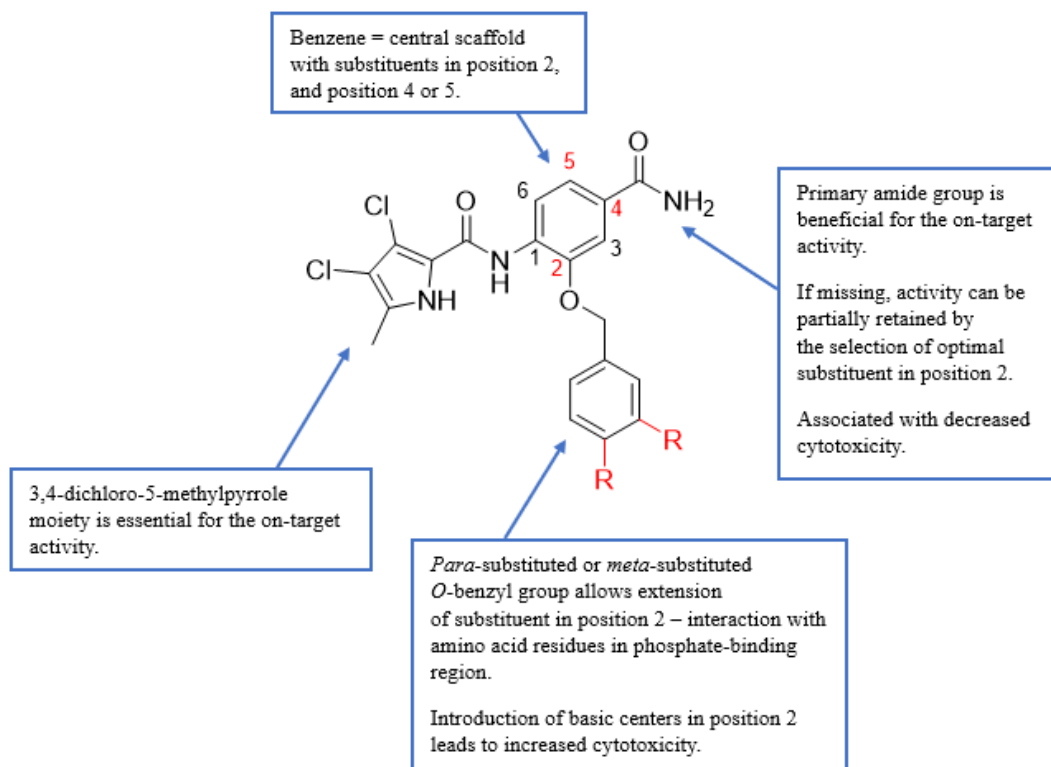*Fig. 20 Structure-activity relationship of the most potent N-Phenylpyrrolamides from the latest study.*

3. Experimental part

The reactions were monitored using TLC and HPLC-MS.

The reagents were obtained from Fluorochem, Asta-Tech, Sigma-Aldrich, Apollo Scientific and Combi-Blocks and they were used without further purification. Solvents were obtained from Merck, Gram-Mol and Carlo Erba.
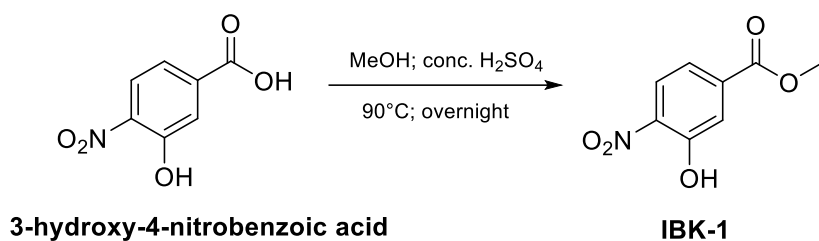
3.1 Synthesis of IBK-12 – reaction scheme

IBK-12 was prepared via multi-step synthesis (Scheme 1) and the product was purified to allow further *in vitro* testing.
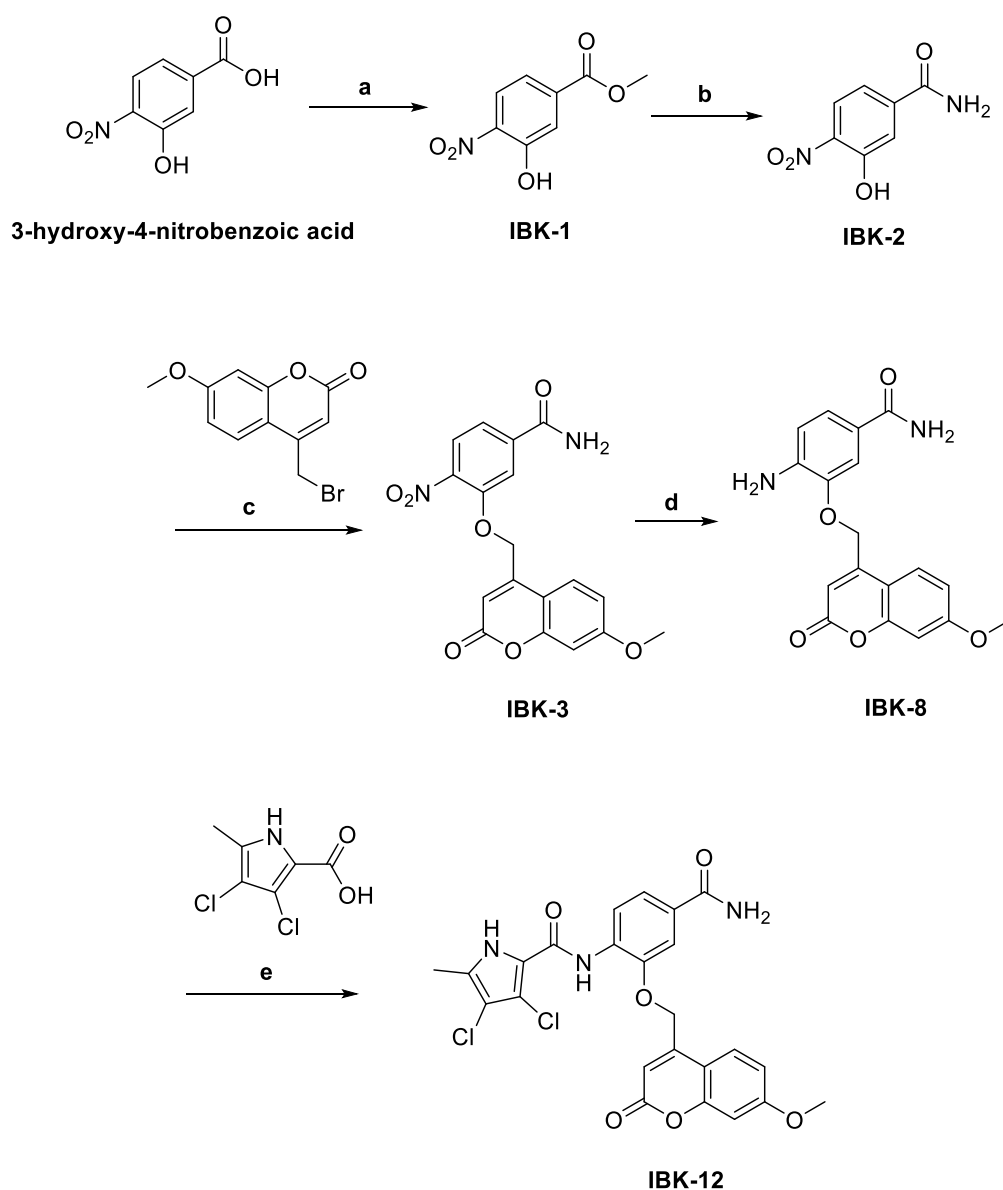
Scheme 1 Reaction scheme – synthesis of IBK-12.
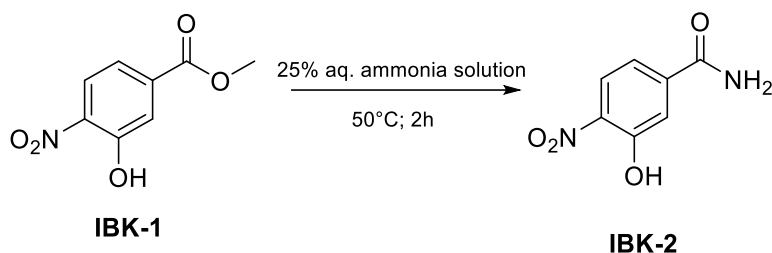
3.1.1 Synthesis of IBK-1

Scheme 2 Synthesis of IBK-1 (esterification).

Scheme 2 represents synthesis of IBK-1 starting from 3-hydroxy-4-nitrobenzoic acid.

3-hydroxy-4-nitrobenzoic acid (46.4 mmol) was dissolved in MeOH (2 mL/mmol) and H_2SO_4 (0.2 mL/mol) was added to this solution dropwise. Reaction mixture was stirred overnight at 90°C under reflux. Then, the reaction mixture was cooled down to room temperature and water was added. Yellow precipitate formed in the flask, and it was filtered off. The precipitate was dried in the oven at 55°C overnight to obtain the product as a yellow solid.

The reaction's progress was monitored by TLC with DCM:MeOH 9:1 as a mobile phase. TLC plate showed no starting material or impurity. HPLC-MS was performed. Yield of the reaction was 98 %.

3.1.2 Synthesis of IBK-2

Scheme 3 Synthesis of IBK-2 (ammonolysis).

Scheme 3 shows synthesis of IBK-2 from previously prepared IBK-1. IBK-1 was used for synthesis of IBK-2 without preceding purification.

IBK-1 (45.66 mmol) was dissolved in 25% aqueous ammonia solution (5 mL/mmol) and resulting yellow solution was stirred at 50 °C. After 1 hour, orange precipitate formed in the reaction mixture. The reaction was monitored using TLC (mobile phase DCM:MeOH 9:1). After 2 hours, no more starting material was visible on the TLC plate, therefore the mixture was cooled down to room temperature and acidified with concentrated HCl till pH 3 was achieved. Orange precipitate changed color to yellow and it was filtered off and washed well with water. The precipitate was dried in the oven at 55°C to obtain the product as a yellow powder.

One more TLC was done using DCM:MeOH 9:1 as a mobile phase. TLC plate was sprayed with ninhydrin solution and gently heated to reassure that all the ammonium chloride that formed in the reaction mixture was washed out with water during isolation step. Ninhydrin, when heated, creates a purple complex with amines. If ammonium chloride was present in the sample and therefore on the TLC plate, it would appear as a purple stain on the plate (Fig. 21).
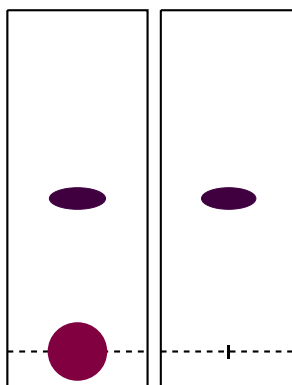
Fig. 21 Schematically depicted difference between a sample containing ammonium chloride (on the left) and a sample that does not contain ammonium chloride (on the right) – TCL treated with ninhydrin solution.

HPLC-MS was performed showing 96% peak of the product and 4% peak of 3-hydroxy-4-nitrobenzoic acid ($\lambda = 254$ nm). Yield of the reaction was 71 %.

To obtain purer product, which turned out to be important for synthesis of IBK-3, yellow precipitate was dissolved in 100 mL of 5% NaHCO$_3$ solution (pH 8) and this solution was extracted three times with 100mL of ethyl acetate. The organic phase was washed with water, with brine, dried over anhydrous Na$_2$SO$_4$ and evaporated under reduced pressure. The resulting orange powder was dried in the oven at 55°C overnight to remove the remaining ethyl acetate. Yield of the pure product after the extraction was 40 %. HPLC-MS was performed showing 100% peak of the product ($\lambda = 254$ nm).

3.1.3 Synthesis of IBK-3

This reaction was repeated three times under different conditions to obtain the desired product. Individual attempts to synthetize IBK-3 are depicted in Scheme 4, Scheme 5, and Scheme 6.

3.1.3.1 IBK-3 – first attempt
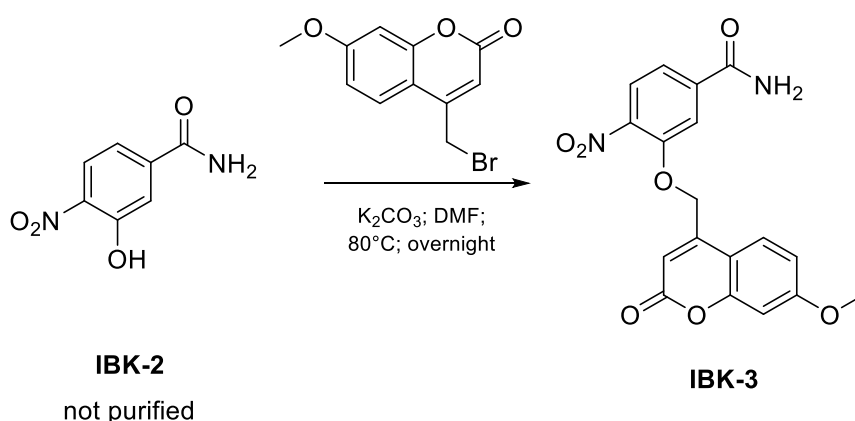
Scheme 4 Synthesis of IBK-3 – first attempt.

IBK-2 (1 mmol; not purified) was dissolved in DMF (2–8 mL/mmol) stored with molecular sieve. To the solution K_2CO_3 (2 eq.) and alkylhalogenide (4-(bromomethyl)-7-methoxy-2*H*-chromen-2-one; 1.1 eq.) were added and the solution was stirred at 80°C overnight protected from light.

Overnight orange reaction mixture changed color to black. On the TLC (mobile phase DCM:MeOH 9:1) there were many visible spots. HPLC-MS was performed showing many peaks at 254 nm (Fig. 22).
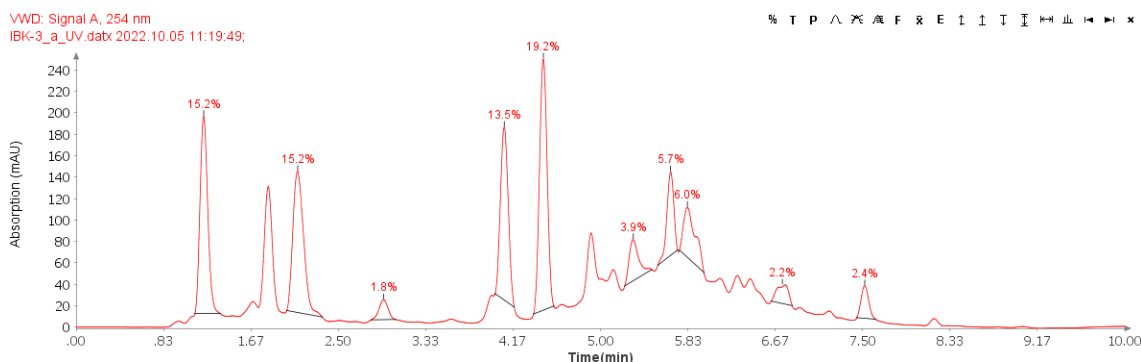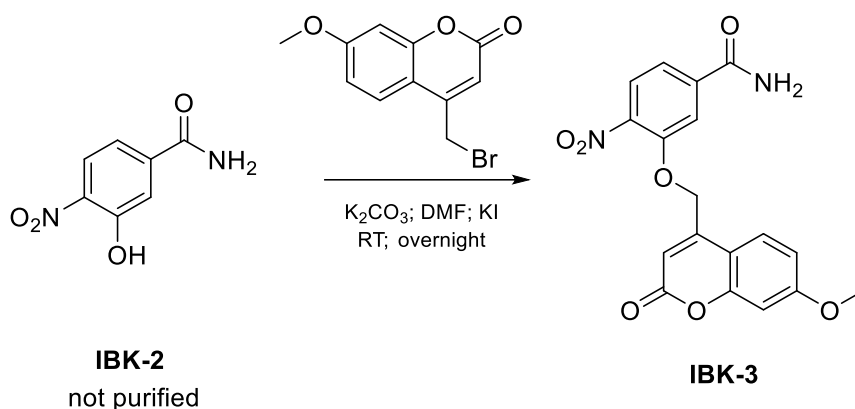

Fig. 22 IBK-3 was not detected among many impurities.

The product was not detected by mass spectrometer therefore the reaction was repeated under slightly modified conditions.

Scheme 5 Synthesis of IBK-3 – second attempt.

IBK-2 (1 mmol; not purified) was dissolved in DMF (2–8 ml/mmol) stored with molecular sieve. To the solution K_2CO_3 (2 eq.), three grains (around 5 mg) of KI as an *in situ* catalyst and alkylhalogenide (4-(bromomethyl)-7-methoxy-2*H*-chromen-2 one; 1.1 eq.) were added and the solution was stirred at room temperature overnight protected from light.

Overnight orange reaction mixture changed color to brown. On the TLC (mobile phase DCM:MeOH 9:1) were many visible spots. Reaction mixture was acidified with 1M HCl till pH 5 was achieved and precipitate was filtered off and washed with water. HPLC-MS was performed (Fig. 23), and IBK-3 was detected by mass spectrometer.
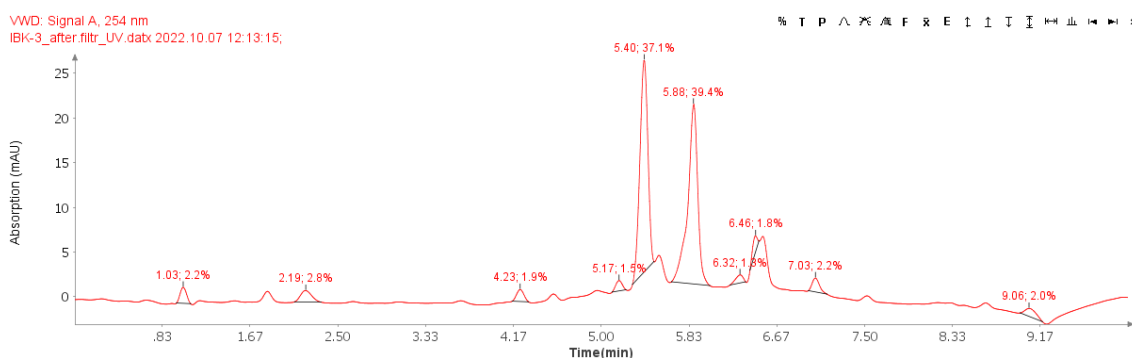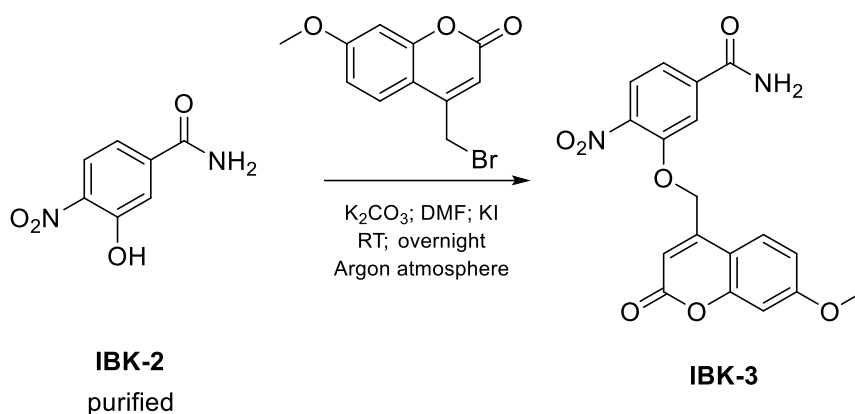

Fig. 23 IBK-3 was detected by mass spectrometry. Under 254 nm UV the product was visible as peak with retention time 5.40 min.

All of many attempts to purify this reaction mixture by column chromatography, recrystallization or collecting precipitate using a centrifuge failed.

3.1.3.3 IBK-3 – third attempt

Scheme 6 Synthesis of IBK-3 – third attempt (etherification).

Reaction was repeated with special attention on protecting the reaction mixture from moisture. The flask used for this reaction was pre-dried in oven at 55°C for 1 hour as well as purified starting compound IBK-2.

IBK-2 (1 mmol; purified) was dissolved in DMF (2–8 ml/mmol) stored with molecular sieve. To the solution K_2CO_3 (2 eq.), three grains (around 5 mg) of KI as an *in situ* catalyst and alkylhalogenide (4-(bromomethyl)-7-methoxy-2*H*-chromen-2-one; 1.1 eq.) were added and the solution was stirred at room temperature overnight under argon atmosphere and protected from light.

Overnight white precipitate formed in the flask. Reaction mixture was acidified with 1M HCl till pH 5 was achieved and precipitate was filtered off and washed with water. Precipitate was dried in the oven at 55°C overnight to obtain the product as a white solid with 96 % yield. HPLC-MS was performed (Fig. 24), IBK-3 was detected by mass spectrometer and ^{1}H NMR was done to confirm the structure.
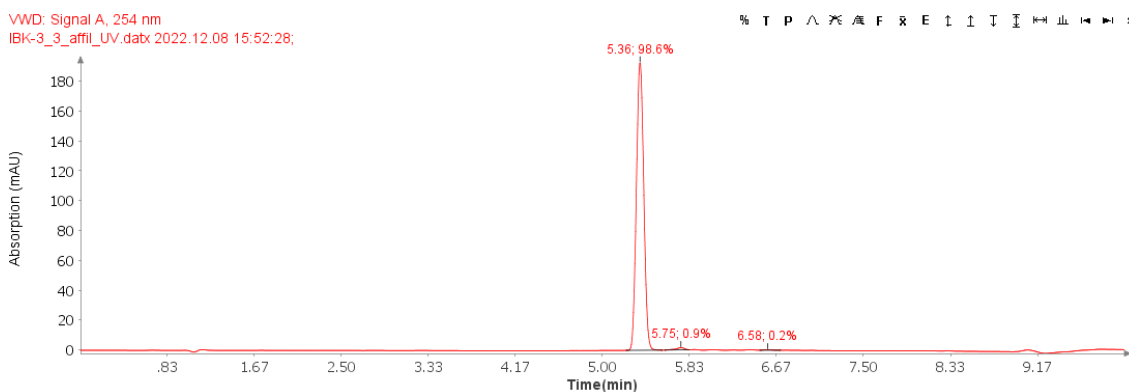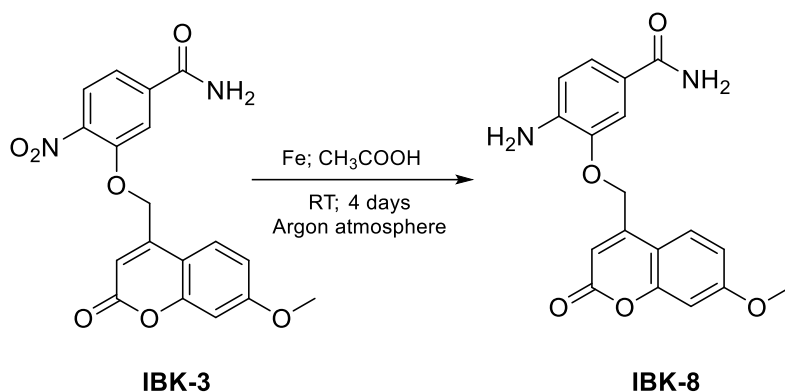

Fig. 24 IBK-3 under 254 nm UV.
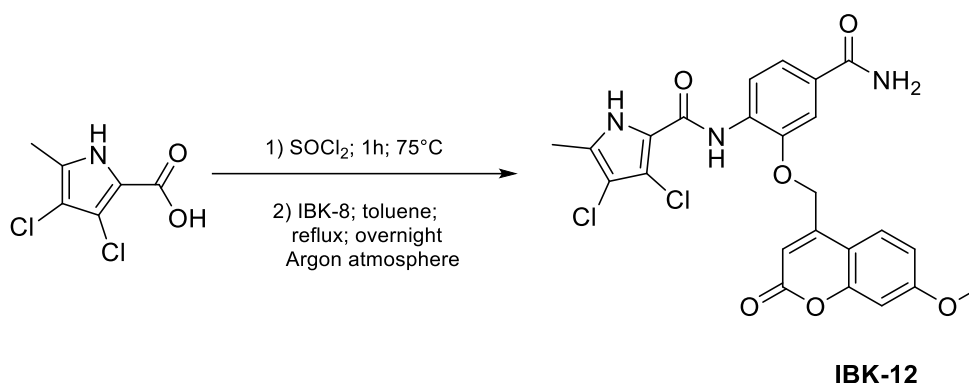
3.1.4 Synthesis of IBK-8

Scheme 7 Synthesis of IBK-8 (reduction).

Scheme 7 represents synthesis of IBK-8. IBK-3, as a product of the previous reaction, was used in this step without preceding purification.

To a stirring solution of IBK-3 (0.919 mmol) in glacial acetic acid (10 mL/mmol), 10 equivalents of powdered iron were added. The reaction mixture was stirred at room temperature overnight under argon atmosphere protected from light. TLC was not convenient for monitoring this reaction since the spot representing starting compound and the spot representing product have similar retention times (mobile phase DCM:MeOH 9:1). Therefore, the reaction was monitored using HPLC-MS. The next day in the morning, 10 more equivalents of powdered iron were added to help the reaction progress faster because HPLC-MS showed 70% peak of the starting compound. Reaction was monitored for four days. After four days the reaction didn't seem to progress anymore, therefore it was stopped, and the product was isolated. The crude was neutralized with 25% aqueous ammonia solution, transferred to separating funnel and extracted with ethyl acetate (10x100 mL). Organic phase was then washed with brine, dried over anhydrous Na_2SO_4 and concentrated under reduced pressure to obtain the product as a white powder with yield 46 %.

3.1.5 Synthesis of IBK-12

Scheme 8 Synthesis of IBK-12 (coupling with carboxylic acid).

Preparation of the final product (IBK-12) is depicted in Scheme 8.

1) 0.52 mmol of 3,4-dichloro-5-methyl-1*H*-pyrrole-2-carboxylic acid (1.2 eq.) and SOCl₂ (2.5 mL/mmol) were stirred at 75°C under argon atmosphere. After one hour SOCl₂ was evaporated using water pump and dried under vacuo.

2) To a flask with activated acid, IBK-8 (1 eq.; 0.43 mmol) was added. Toluene was added as a solvent and the reaction mixture was heated to 115°C and stirred under condenser under argon atmosphere overnight protected from light.

Toluene evaporated from the reaction mixture overnight and dark grey solid stayed in the flask. The solid was suspended in DCM and filtered. HPLC was performed and starting compound IBK-8 was detected, therefore another 28 mg of 3,4-dichloro-5-methyl-1*H*-pyrrole-2-carboxylic acid were activated, added to crude from previous reaction, toluene was added as a solvent and the reaction mixture was heated to 115°C again and left under reflux under argon atmosphere overnight protected from light. Overnight, toluene evaporated again, and grey solid stayed in the flask. The solid was suspended in DCM and filtered. HPLC-MS was done, and no more starting compound was detected.

To remove the excess acid from reaction mixture, the solid was suspended in saturated solution of NaHCO₃ (pH 8–9) hoping that the acid would create a water-soluble salt. This approach failed therefore the solid was suspended in DCM two more times to remove the excess acid. HPLC-MS was done (Fig. 25) and it showed that there was an impurity in the mixture with very similar retention time as the starting acid.
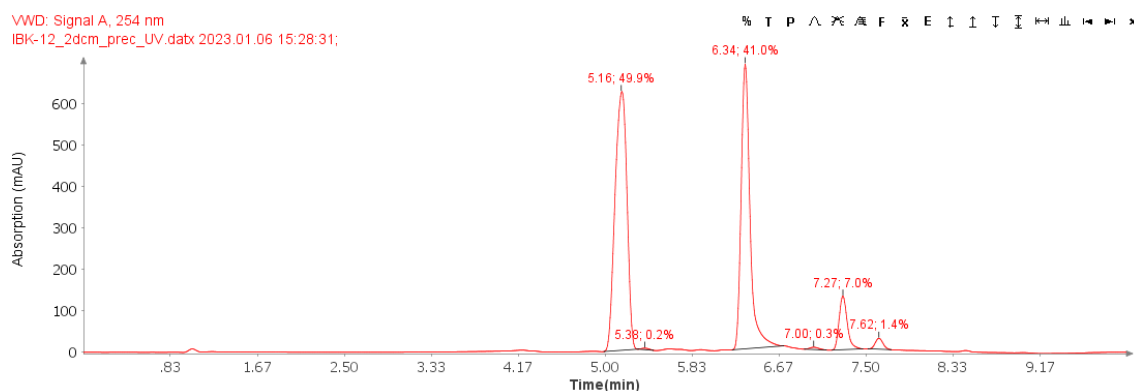
Fig. 25 Peak of an impurity with similar retention time (5.16 min) as the starting acid.

This impurity was also detected using a TLC (DCM:MeOH 15:1). It appeared as a spot with similar properties as the starting acid. On the TLC, the impurity could be distinguished from the starting acid under UV light with 366 nm wavelength – the impurity was visible as a shining blue spot (Fig. 26).
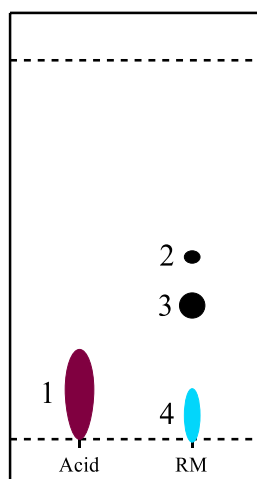

Fig. 26 Starting acid (spot 1); impurity with similar retention time as the starting acid (spot 4); the product (spot 3); another impurity (spot 2). Mobile phase DCM:MeOH 15:1.

The reaction mixture was purified using column chromatography. As a mobile phase, DCM:MeOH 15:1 was used. Test tubes with eluate were examined using TLC and HPLC-MS, and the results showed that the purification was not completely successful. Test tubes with the least impurities were joined into one fraction, mobile phase was evaporated and the solid was prepared for another column chromatography. This time DCM:MeOH 19:1 was used as a mobile phase. Purification was successful, around 3 mg of the product were obtained, the product was detected with mass spectrometer, ^{1}H NMR was done to confirm the structure and the product was later tested for inhibitory activity on hTopoIIα using relaxation assay kits.
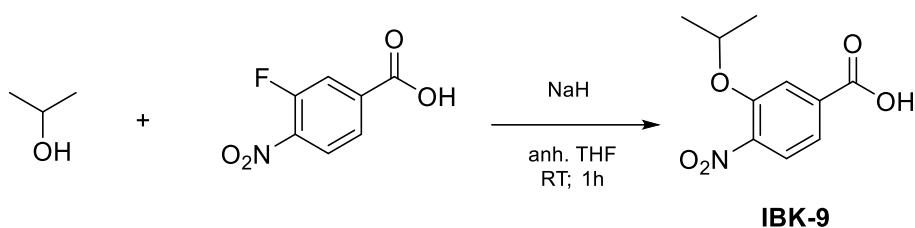
3.2 Synthesis of IBK-11 – reaction scheme

IBK-11 was intended to be prepared via multi-step synthesis (Scheme 9). Preparation of the final compound failed in the last step of synthesis.
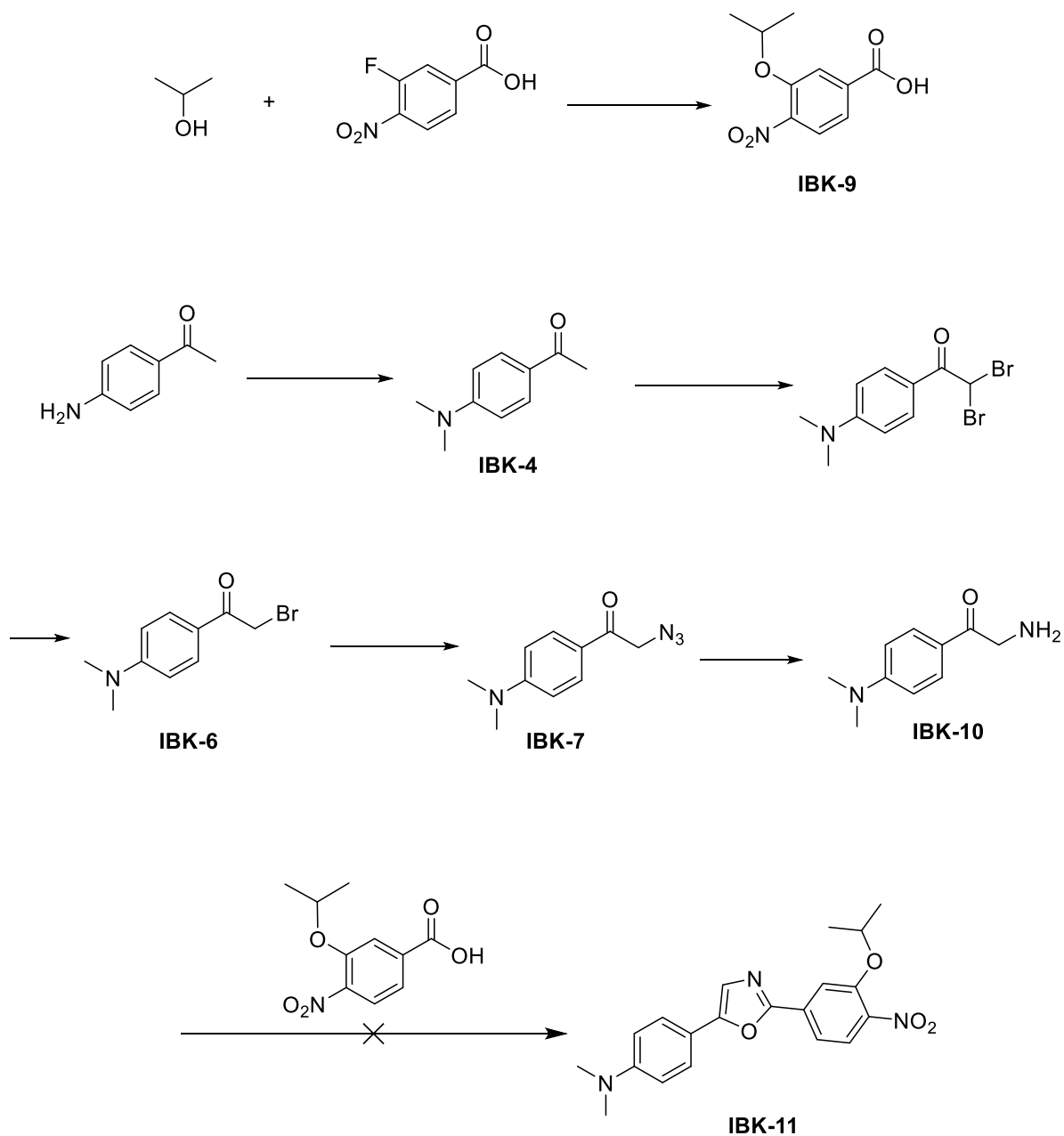
Scheme 9 Reaction scheme – synthesis of IBK-11.
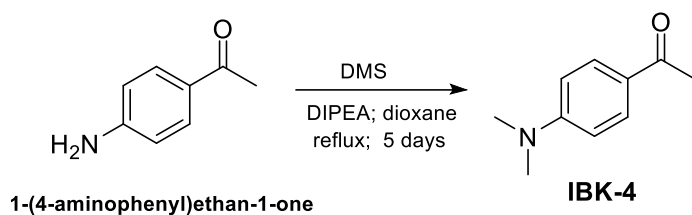
3.2.1 Synthesis of IBK-9

Scheme 10 Synthesis of IBK-9.

Scheme 10 represents synthesis of IBK-9 which was later used as one of the starting compounds for synthesis of IBK-11.

NaH 60% dispersion in mineral oil (27 mmol; 2.5 eq.) was put in a 100 mL flask and 20 mL of anhydrous THF were added. The resulting solution was stirred on ice under argon. A mixture of isopropanol (11.9 mmol; 1.1 eq.) and anhydrous THF was added to the flask using a dropper. The resulting mixture was left stirring on ice under argon for 15 minutes. 3-fluoro-4-nitrobenzoic acid (10.8 mmol; 1 eq.) was added to the reaction mixture in four portions over 10 minutes at 0 °C with rapid stirring (reaction mixture changed color to black). The reaction mixture was stirred at 0 °C for another 15 minutes and then it was stirred at room temperature for 1 hour. After 1 hour, HPLC-MS was done to prove that the reaction was completed.

Saturated NH_4Cl (2 mL/mmol) was added, and the reaction mixture was poured into 100 mL of ethyl acetate and extracted in separating funnel. The organic layer was washed with 1M HCl (3x40 mL), water (40 mL) and brine (40 mL). The organic layer was dried with anhydrous Na_2SO_4 and evaporated to obtain product as a sweet-smelling light brown solid with yield 98 %.

3.2.2 Synthesis of IBK-4

Scheme 11 Synthesis of IBK-4.

Scheme 11 represents synthesis of IBK-4 from the starting 1-(4-aminophenyl)ethan-1-one. Due to complicated preparation and purification of IBK-4 and low yield of this reaction, store-bought 4-dimethylaminoacetophenone was used for the next step – synthesis of IBK-6.

A mixture of 1-(4-aminophenyl)ethan-1-one (71 mmol), dimethyl sulfate (156.2 mmol), diisopropylethylamine (156.2 mmol) and 70 ml of dioxane was refluxed for 5 days. Reaction was monitored using TLC (mobile phase hexane:ethyl acetate 1:1) and HPLC-MS. After 5 days, the reaction stopped progressing therefore it was cooled down to room temperature. 15 mL of dimethyl sulfate were added, and the reaction was heated again. Reaction was refluxed overnight and after that it was stopped, because newly formed impurities were detected by HPLC-MS.

Water was added to the reaction mixture and the reaction mixture changed to dark oily viscose liquid. Dioxane was evaporated from the mixture under reduced pressure and the remaining water phase was extracted with DCM. Organic phase was dried over anhydrous Na_2SO_4 and evaporated and brown oily crude stayed in the flask. Overnight this crude solidified. According to TLC (mobile phase DCM:MeOH 149:1) and HPLC-MS the crude was not pure, therefore purification followed as a next step.

Chromatography column was prepared, the crude was dissolved in DCM and introduced to the prepared column. 100 mL of DCM was poured over the crude solution and fraction number 1 was collected to Erlenmeyer flask. To obtain fraction number 2, 100 mL of DCM:MeOH 150:1 was used as a mobile phase. 100 mL of DCM:MeOH 100:1 was used to obtain fraction number 3, 100 mL of DCM:MeOH 50:1 to obtain fraction number 4 and 100 mL of DCM:MeOH 9:1 to obtain fraction number 5. TLC and HPLC-MS showed that none of the fractions was pure.

Fraction number 1 was taken, since it contained most of the product and least of impurities, and it was evaporated under reduced pressure to obtain yellow solid. The solid was recrystallized from water:MeOH 1:1. Crystals were filtered and dried at 55°C. HPLC-MS was performed. The product was obtained as a yellow solid with yield 10 %.

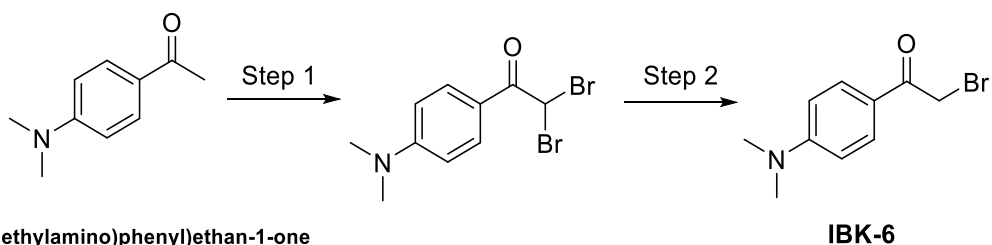## 3.2.3 Synthesis of IBK-6

3.2.3.1 IBK-6 – first attempt

1-(4-(dimethylamino)phenyl)ethan-1-one   **IBK-6**
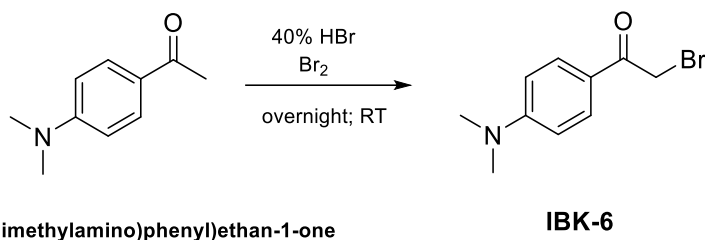
Scheme 12 Synthesis of IBK-6 – first attempt.

Scheme 12 represents synthesis of IBK-6 using 40% hydrobromic acid as a solvent. This reaction was later discontinued due to significant amount of impurities and different approach was chosen for obtaining the desired product.

4-dimethylaminoacetophenone (13.5 mmol) was dissolved in 4.5 mL of 40% hydrobromic acid and treated with a solution of bromine (590 µl) in 2.8 mL of 40% hydrobromic acid over 15 minutes and the mixture was stirred overnight at 20°C. Reaction changed color from orange to yellow solution in around 10 minutes.

In the morning, HPLC-MS was done, and four peaks were detected by HPLC at 254 nm. According to the obtained data, the reaction stopped proceeding therefore three more drops of bromine were added to see if the reaction will progress. After six more hours another HPLC-MS was performed, and it confirmed that the reaction did not progress anymore, therefore it was stopped. Due to significant amount of impurities in the reaction mixture it was decided that different approach would be used to obtain the desired product. For that reason, the reaction mixture was left unpurified.

3.2.3.2 IBK-6 – second attempt

1-(4-(dimethylamino)phenyl)ethan-1-one   **IBK-6**

Scheme 13 Synthesis of IBK-6 – second attempt.

Approach depicted in Scheme 13 was adapted from Diwu et al.[38]

Step 1: 4-dimethylaminoacetophenone (12.3 mmol) was dissolved in 12 mL of concentrated H_2SO_4 and the resulting solution was cooled to 0 °C. Bromine (12.8 mmol)

was slowly added to the solution at 0 °C with rapid stirring. The mixture was gradually warmed to room temperature and stirred overnight. In the morning, the progress of the reaction was inspected using TLC (mobile phase DCM) and HPLC-MS. Small amount of starting compound was detected but in next hours the reaction did not progress any further therefore it was stopped.

The reaction mixture was poured into ice/water and green precipitate formed. The precipitate was collected by filtration, washed with water, and air-dried. HPLC-MS was performed showing that the starting compound was removed from the reaction mixture by isolation step. One impurity was detected by HPLC-MS (Fig. 27). According to data from mass spectrometer the impurity is suggested to be tribrominated starting compound. Yield of the reaction was 72 % with no further purification.
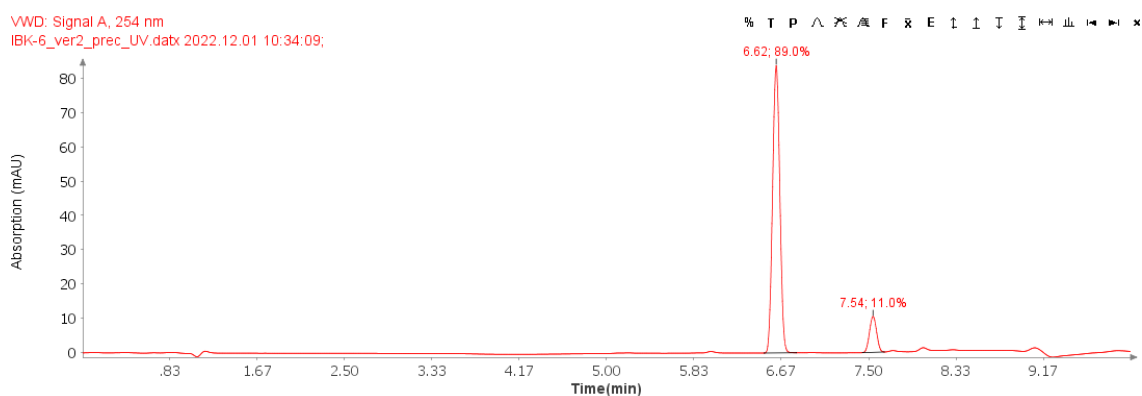
Fig. 27

Brominated compounds show specific pattern in mass spectrum as a consequence of bromine naturally existing almost equally in two isotopic forms – ^{79}Br and ^{81}Br.[39] Therefore, monobrominated compounds generate two peaks in mass spectrum reflecting different mass number of each isotope (Fig. 28).
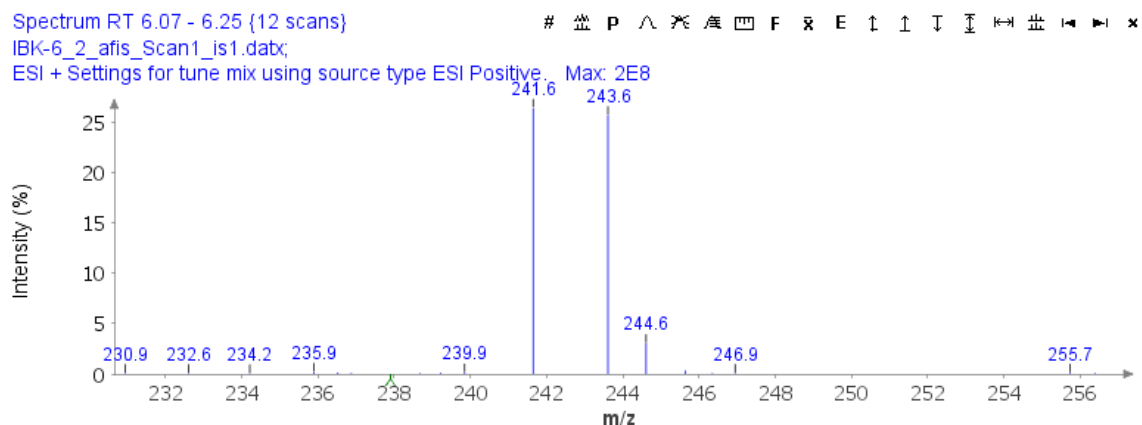

Fig. 28

Step 2: Precipitate from step 1 was dissolved in 12.5 mL of THF and the resulting solution was cooled to 0 °C. To the solution 1.1 mL of diethylphosphite and 1.2 mL of triethylamine in 6.2 mL of THF were added dropwise at 0 °C with stirring. The resulting mixture was warmed to room temperature and stirred for 6 hours. Reaction mixture changed color from green to brown. Reaction was monitored using TLC (mobile phase DCM) and HPLC-MS. After 6 hours the reaction mixture was concentrated in vacuo and poured into ice/water and green precipitate formed. The precipitate was collected by filtration, washed with water and airdried. TLC was done and HPLC-MS was performed showing peaks of 81,6 % monobrominated product and 18,4 % dibrominated compound as an impurity (Fig. 29).
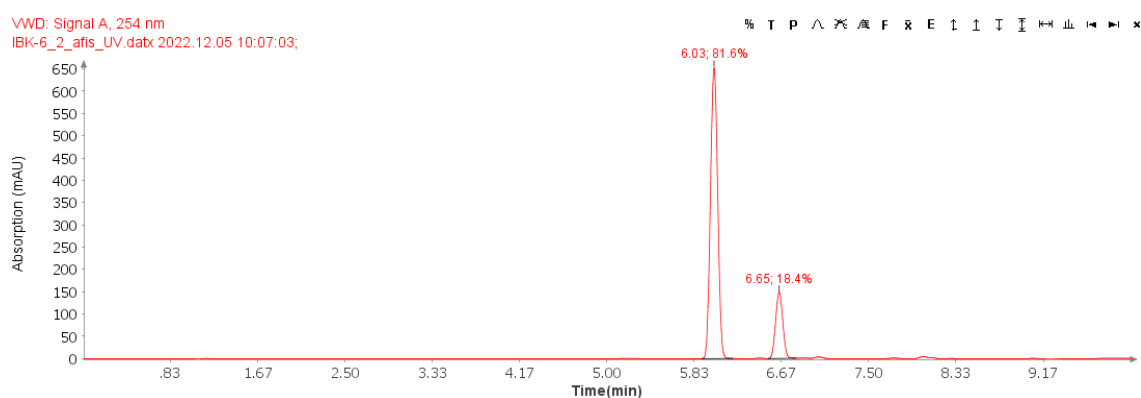

Fig. 29

Yield of unpurified reaction mixture was 58 %. The reaction mixture was purified by column chromatography using DCM as a mobile phase. Yield of pure product after column chromatography was 23 %.

The whole process was later repeated with yields: 78 % after step 1, 54 % of unpurified reaction mixture after step 2, and 19 % of pure product after column chromatography.

3.2.4 Synthesis of IBK-7
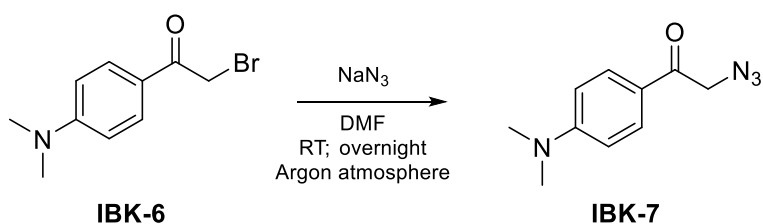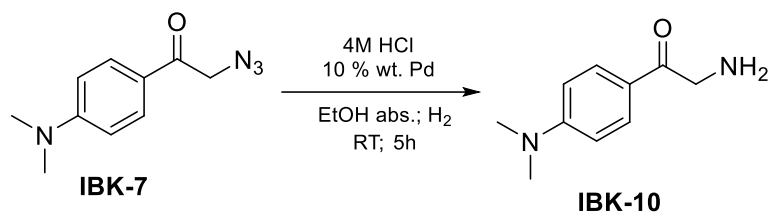

Scheme 14 Synthesis of IBK-7.

Scheme 14 represents preparation of IBK-7. Purified IBK-6 from the previous reaction was used in this step.

IBK-6 (1.3 mmol; 1 eq.) was put in a flask and 5 mL of DMF were added. To this reaction mixture NaN_3 (1.7 mmol; 1.3 eq.) was added in one portion and the mixture was stirred at room temperature overnight under argon atmosphere. Reaction mixture changed color from green to brown. Reaction was monitored with TLC (mobile phase DCM) and HPLC-MS.

After diluting reaction mixture with water red precipitate formed. The precipitate was extracted between water and hexane/ether 1:1 (3x10 mL of organic phase and then 2x100 mL of organic phase). Organic phase was evaporated under reduced pressure to obtain product as an orange solid with yield 69 %. ^{1}H NMR was done to confirm structure of the product.

Later this reaction was repeated with yield 69 %.
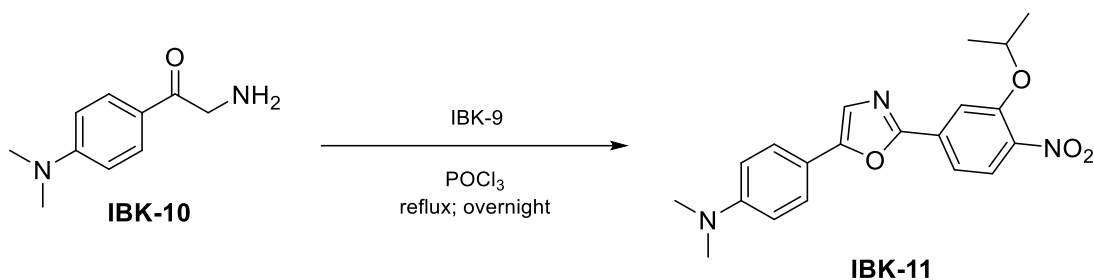
3.2.5 Synthesis of IBK-10

Scheme 15 Synthesis of IBK-10.

Scheme 15 represents synthesis of IBK-10 via catalytic hydrogenation.

The product was prepared using standard catalytic hydrogenation procedure. IBK-7 (0.9 mmol) was dissolved in EtOH absolute (around 50 mL) in 100 mL two-necked flask. 1 mL of 4M HCl in dioxane was added to flask under argon atmosphere. 10 % wt. of Pd (18.5 mg) was added to the flask and H_2 was left bubbling through the reaction mixture. The progress of catalytic hydrogenation was monitored with HPLC-MS every hour. The reaction was finished after five hours. The reaction mixture was filtered using 0.45µm HPLC filter to remove Pd. Acquired solution was evaporated under reduced pressure.

To obtain amine from the yielded ammonium salt (chloride), the crude was dissolved in 100 mL of water (result was yellow/brown solution with pH 3). Water phase was extracted with 10 mL of DCM and then it was neutralized with saturated $NaHCO_3$ solution (color of the solution changed to red). Water phase was extracted four times with 20 mL of DCM until it remained colorless. Organic phase was dried with anhydrous Na_2SO_4 and evaporated. The product was obtained as red solid with yield 62 %.

3.2.6 Synthesis of IBK-11

Scheme 16 Synthesis of IBK-11.

Scheme 16 represents unsuccessful synthesis of final compound IBK-11.

A mixture of IBK-10 (0.56 mmol; 1 eq.), IBK-9 (0.92x0.56 = 0.52 mmol; 1 eq.) and 1 mL of phosphorus oxychloride was refluxed overnight. The next day, reaction was not finished according to the data from HPLC-MS (Fig. 30), therefore it was left under condenser over the weekend.
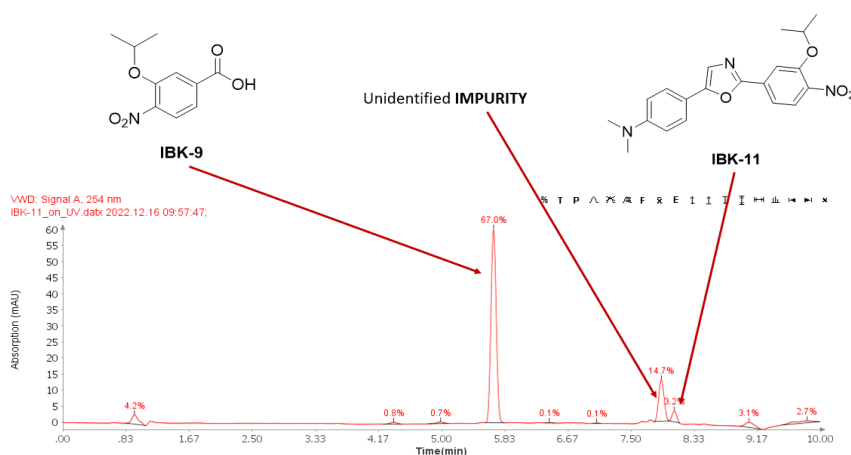

Fig. 30 Data from HPLC (detection under 254 nm) showing starting compound IBK-9, the main impurity, and a small peak of the product.

After the weekend, HPLC-MS was done showing many peaks which suggested that the reactants decomposed in the reaction mixture. Reaction mixture was cooled down to room temperature and quenched with ice cold water. Mixture was neutralized with saturated NaHCO$_3$ solution and extracted with ethyl acetate. After evaporating organic phase, 20 mg of crude stayed in the flask. The crude was recrystallized from 30 mL of MeOH to obtain a small amount of not desired compound (dark brown solid). HPLC-MS was performed with this compound showing one main peak under 254 nm UV. The aim was to prepare sample of this impurity for ^{1}H NMR, but this task was not successfully accomplished due to poor solubility of the sample. The impurity was not further identified.
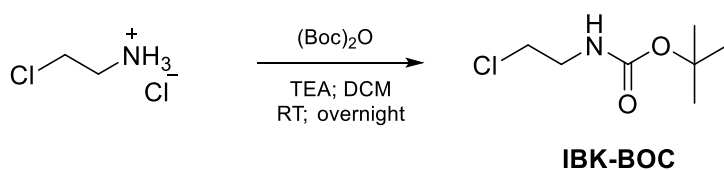
3.3 Synthesis of IBK-5 – reaction scheme

Intended synthesis of a compound containing BODIPY fluorophore in the structure is shown in Scheme 17. This synthesis failed in a first step.
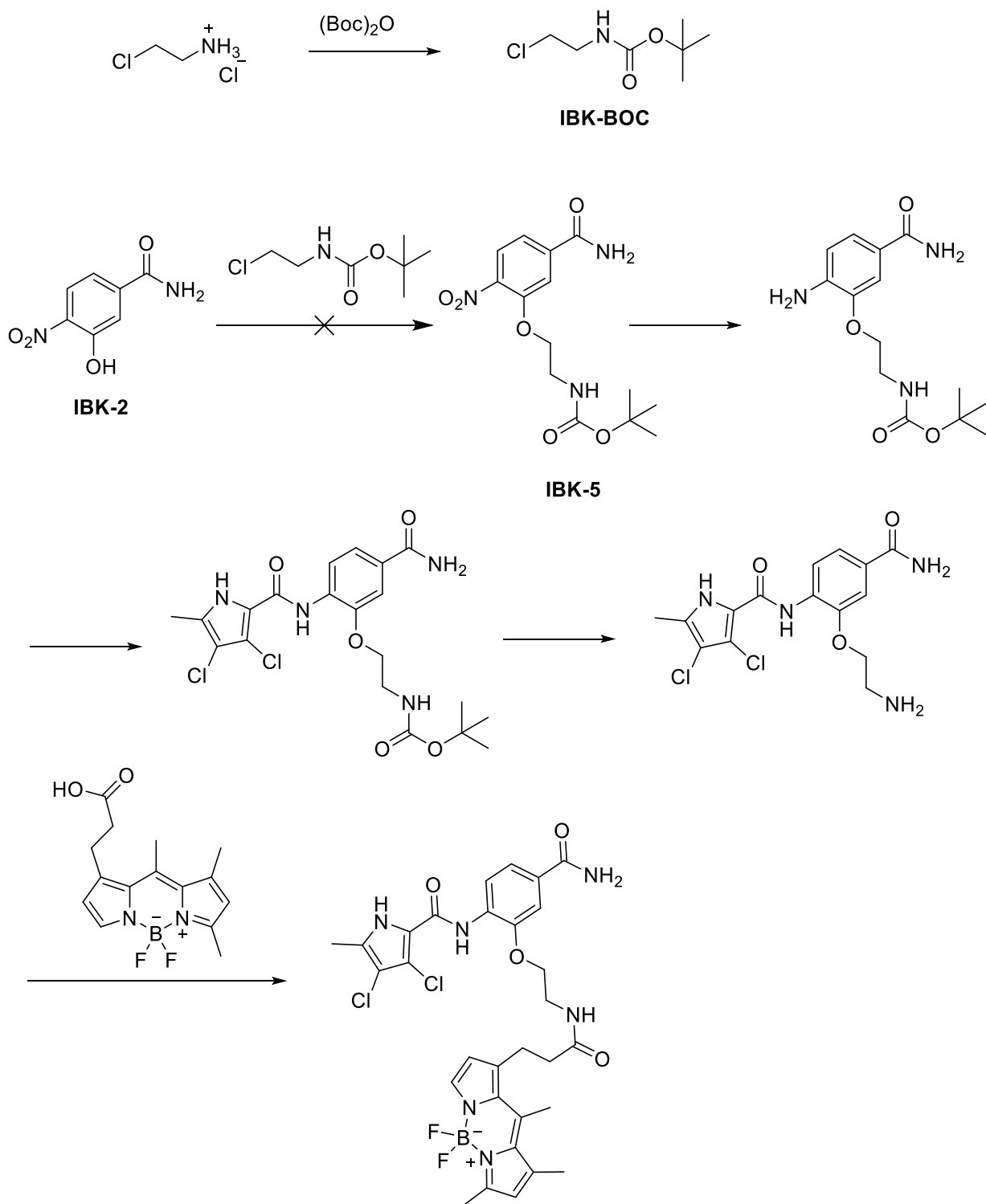
Scheme 17 Unsuccessful preparation of compound containing BODIPY fluorophore.
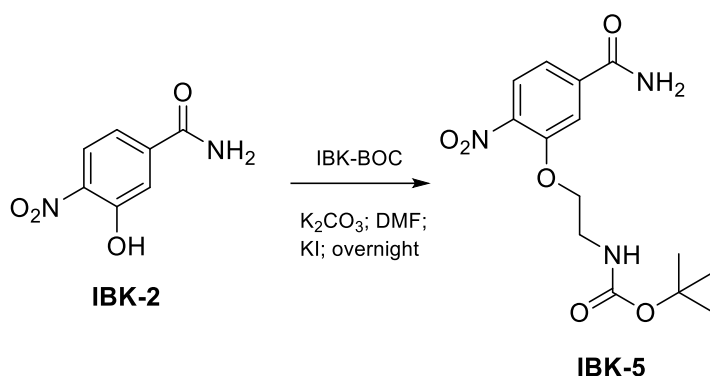
3.3.1 Synthesis of IBK-BOC

Scheme 18 Synthesis of IBK-BOC.

Preparation of an intermediate necessary for synthesis of IBK-5 is represented in Scheme 18.

41.3 mmol of 2-chloroethylamine was dissolved in DCM and 41.3 mmol of triethylamine was added. Resulting solution was stirred on ice. 35.1 mmol of di-*tert*-butyl dicarbonate was dissolved in DCM and added dropwise to a solution of 2-chloroethylamine on ice which was accompanied by bubbles evolving in the reaction mixture. The resulting mixture was stirred overnight at room temperature. In the morning, TLC was done using DCM and MeOH 9:1 as a mobile phase. TLC plate was sprayed with ninhydrin solution and heated to detect the spots. Product of the reaction was detected therefore the reaction was stopped and product was isolated. Reaction mixture was placed in a separating funnel and washed three times with 50 mL of 5% citric acid solution. Then it was washed with 50 mL of brine and dried over anhydrous Na_2SO_4. The organic phase was evaporated under reduced pressure to obtain the product as a yellow liquid with sharp smell. Yield of the reaction was 84 %.

3.3.2 Synthesis of IBK-5

Scheme 19 Synthesis of IBK-5.

Reaction shown in Scheme 19 was repeated four times under different conditions. However, the product was not successfully isolated after any of performed attempts. Each attempt eventually resulted in very similar outcome (Fig. 31).
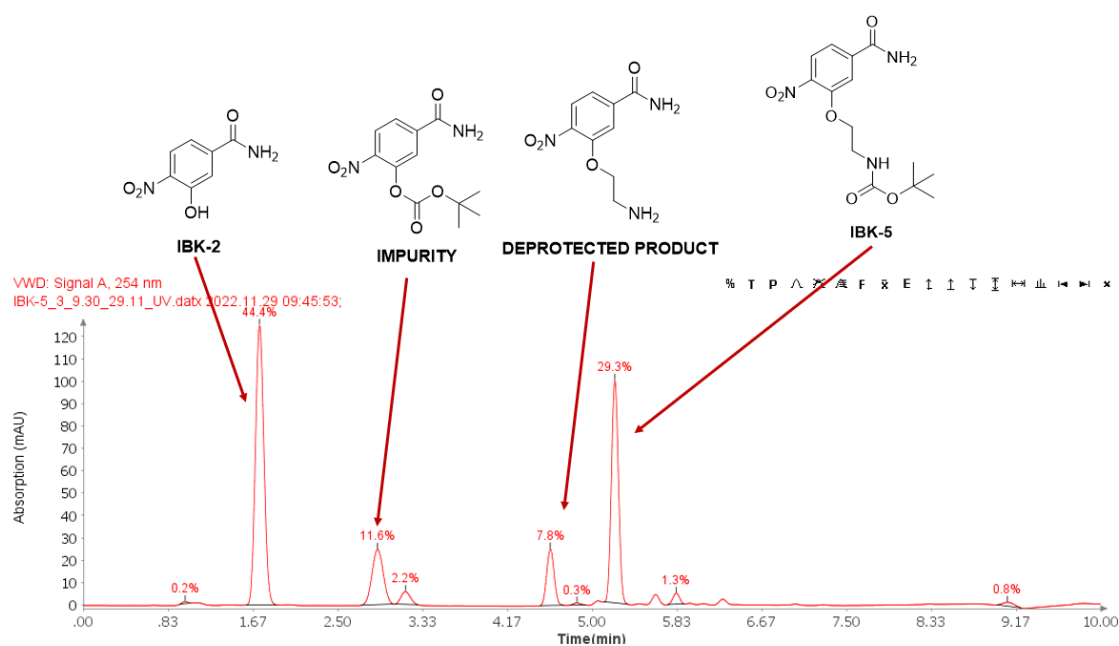

Fig. 31

During the first attempt, unpurified IBK-2 (1.1 mmol) was used as a starting compound. This staring compound was dissolved in DMF (2–8 mL/mmol) stored with molecular sieve. To the solution K_2CO_3 (2 eq.) and IBK-BOC (1.1 eq.) were added, around 3 mg of KI was used as an *in situ* catalyst and the solution was stirred at 80°C overnight. The next day, significant amount of starting compound IBK-2 was detected by HPLC-MS, therefore 0.2 eq. of IBK-BOC were added. The reaction progressed slowly and for this reason 0.4 eq. more of IBK-BOC were added five hours later. The reaction mixture was

stirred at 80°C overnight. The next day, many impurities were detected by HPLC-MS, therefore the reaction was stopped.

For the second attempt, unpurified IBK-2 (1.1 mmol) was used as a starting compound again. This staring compound was dissolved in DMF (2–8 mL/mmol) stored with molecular sieve. To the solution K_2CO_3 (2 eq.) and IBK-BOC (1.1 eq.) were added, around 3 mg of KI was used as an *in situ* catalyst and the solution was stirred at 50°C overnight. The next day, no progress was detected by HPLC-MS, thus the temperature of the reaction mixture was raised to 80°C and the reaction was stirred over the weekend. After the weekend, significant amount of starting compound IBK-2 was detected by HPLC-MS as well as peaks of many impurities. The reaction mixture was heated to 100°C to see whether the reaction would proceed. After six hours of monitoring the reaction by HPLC-MS, only peaks of impurities were magnifying, therefore the reaction was stopped.

During the third attempt, unpurified IBK-2 (1.1 mmol) was used as a starting compound. This staring compound was dissolved in DMF (2–8 mL/mmol) stored with molecular sieve. To the solution K_2CO_3 (2 eq.) and IBK-BOC (1.1 eq.) were added, around 3 mg of KI was used as an *in situ* catalyst and the solution was stirred at 100°C overnight. The next day, significant amount of starting compound IBK-2 was detected by HPLC-MS, therefore 0.2 eq. of IBK-BOC were added. The reaction did not proceed. Therefore, it was stopped and isolation followed as a next step. Reaction mixture was acidified with 1M HCl till pH 5 was achieved and precipitate was filtered off and washed with water. Unfortunately, the product was not isolated from the reaction mixture during this step and the obtained crude consisting of the product and impurities had to undergo purification. Attempts to purify the crude by recrystallization, column chromatography or separating precipitate from the reaction mixture using a centrifuge were not successful and the reaction was repeated one more time.

For the last attempt, purified IBK-2 (1.1 mmol) was used as a starting compound. This staring compound was dissolved in DMF (2–8 mL/mmol) stored with molecular sieve. To the solution K_2CO_3 (2 eq.) and IBK-BOC (1.1 eq.) were added, around 3 mg of KI was used as an *in situ* catalyst and the solution was stirred at room temperature under argon atmosphere for three hours. Since the reaction did not progress at all at room temperature, the temperature was gradually raised to 90°C and the reaction mixture was stirred overnight under argon atmosphere. The next day, many impurities were detected

by HPLC-MS, therefore the reaction was stopped. Attempts to purify the reaction mixture by recrystallization or column chromatography were not successful.

Due to difficulties with synthesis of IBK-5 and problems with subsequent purification, it was decided that preparation if IBK-5 will be discontinued.

Obtained compounds
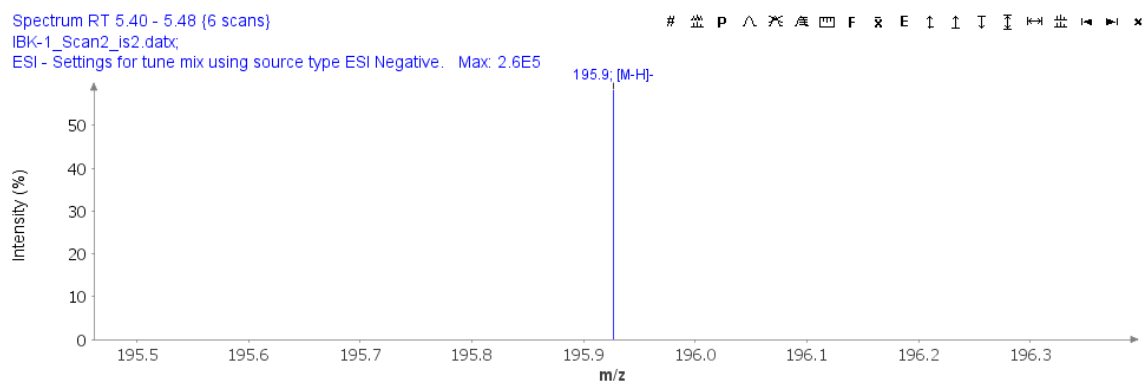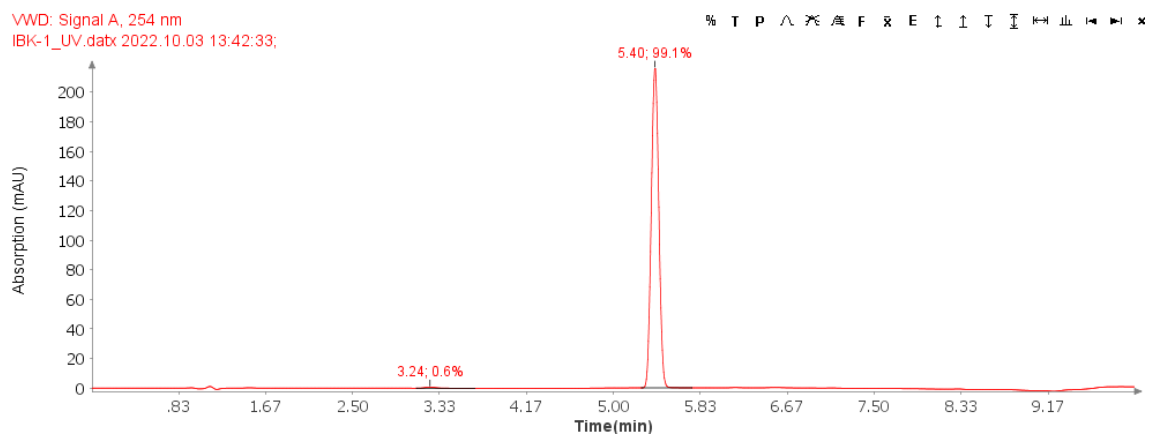
3.4 IBK-1
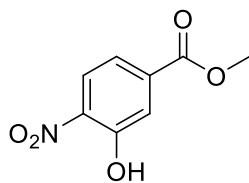
Name: methyl 3-hydroxy-4-nitrobenzoate

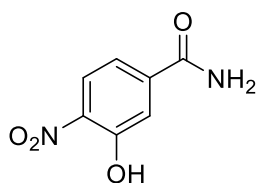**Appearance:** yellow solid

Molecular weight: 197.03 g/mol

Yield: 98 %

Retention factor: 0.80 (DCM:MeOH = 9:1)

HPLC-MS (ESI-, m/z): [M-H]$^-$ 195.9
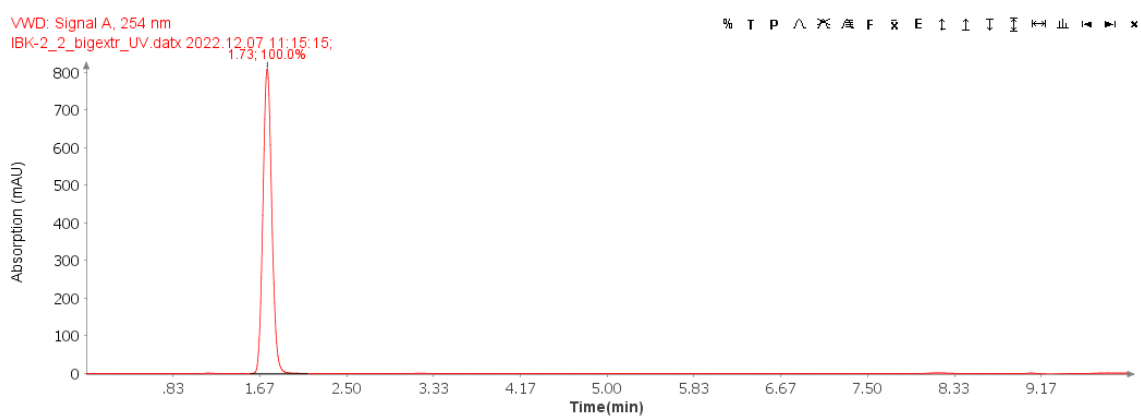
3.5 IBK-2

Name: 3-hydroxy-4-nitrobenzamide

Appearance: orange solid

Molecular weight: 182.03 g/mol

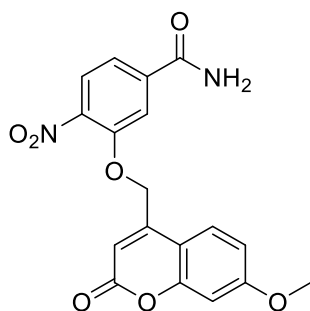**Yield:** 71 % unpurified reaction mixture; 40 % product after purification

Retention factor: 0.40 (DCM:MeOH = 9:1)

HPLC-MS (ESI-, m/z): [M-H]$^-$ 180.9
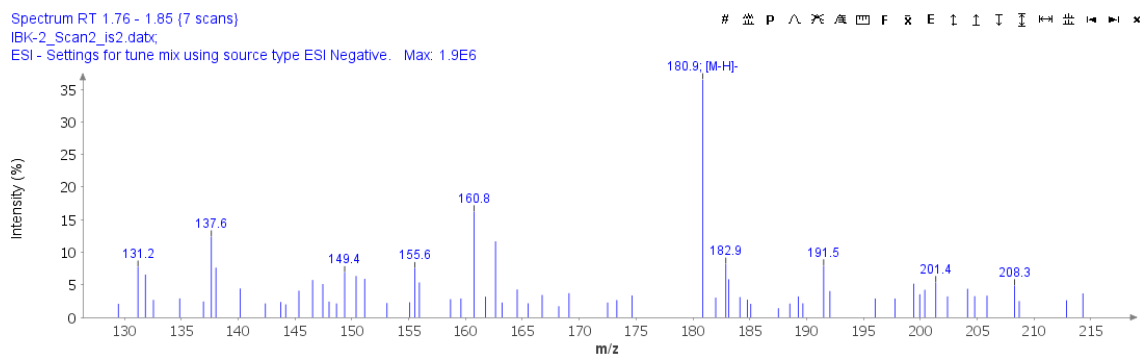
^{1}**H NMR** (400 MHz, DMSO) δ 11.21 (s, 1H), 8.15 (s, 1H), 7.93 (d, J = 8.5 Hz, 1H), 7.63 (s, 1H), 7.56 (d, J = 1.7 Hz, 1H), 7.39 (dd, J = 8.5, 1.8 Hz, 1H)

3.6 IBK-3

Name: 3-((7-methoxy-2-oxo-2*H*-chromen-4-yl)methoxy)-4-nitrobenzamide

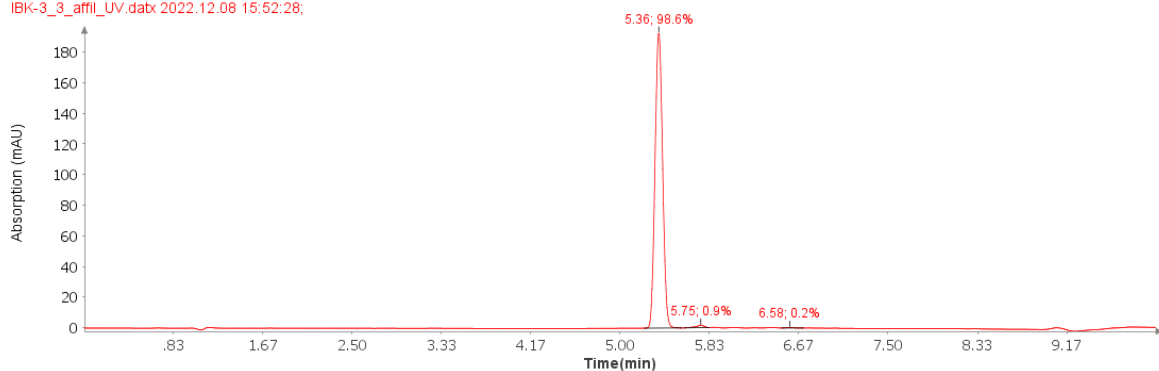**Appearance:** white solid (supposedly photosensitive)

Molecular weight: 370.08 g/mol
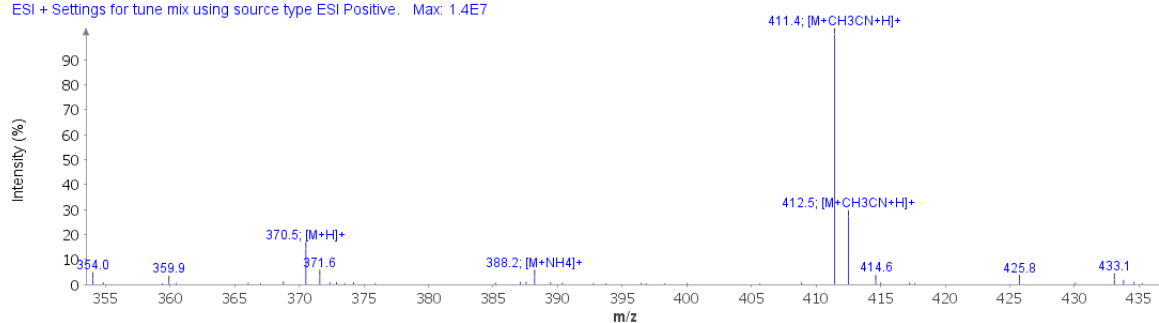
Retention factor: 0.42 (DCM:MeOH = 9:1)

Yield: 96 %

HPLC-MS (ESI+, m/z): $[M+H]^+$ 370.5

^{1}H NMR (400 MHz, DMSO) δ 8.24 (s, 1H), 7.76 (d, J = 9.0 Hz, 1H), 7.66 (d, J = 8.7 Hz, 1H), 7.05 (s, 2H), 6.98 (d, J = 9.1 Hz, 2H), 6.28 (s, 1H), 6.15 (s, 1H), 5.37 (s, 2H), 3.87 (s, 3H)
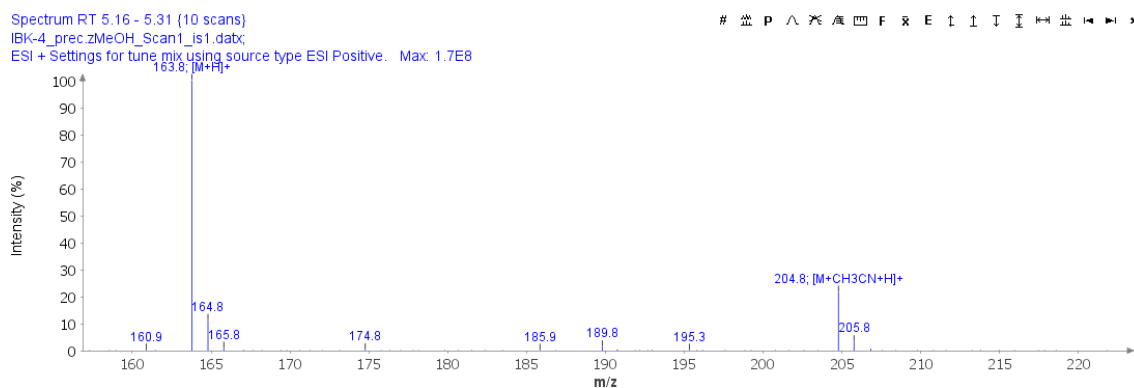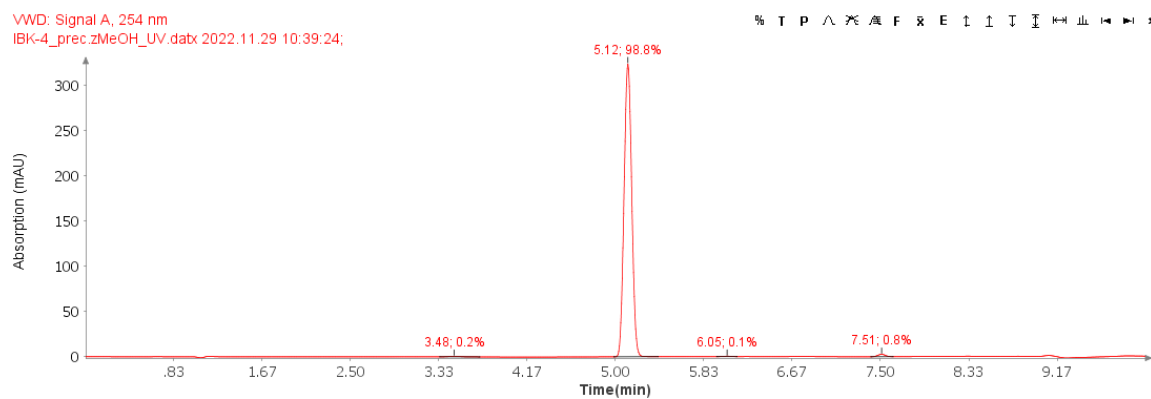
3.7   IBK-4
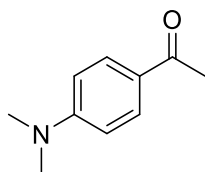
Name: 1-(4-(dimethylamino)phenyl)ethan-1-one

Appearance: light yellow solid

Molecular weight: 163.10 g/mol
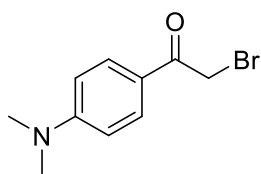
Yield: 10 %

HPLC-MS (ESI+, m/z): [M+H]$^+$ 163.8

3.8 IBK-6

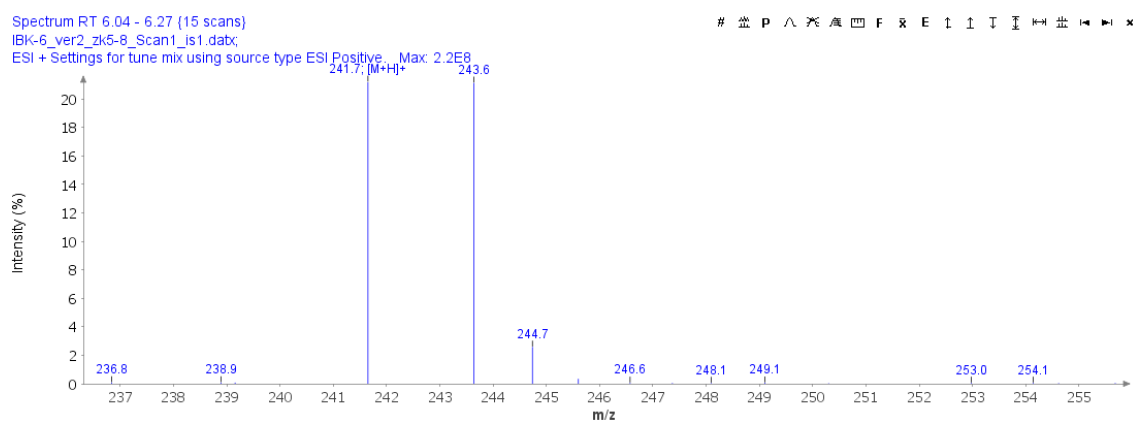**Name:** 2-bromo-1-(4-(dimethylamino)phenyl)ethan-1-one

Appearance: green solid

Molecular weight: 241.01 g/mol

Retention factor: 0.25 (DCM)

Yield: unpurified reaction mixture 58 %; purified product 23 % (resp. 54 % and 19 % after repeating the reaction)

HPLC-MS (ESI+, m/z): $[M+H]^+$ 241.7
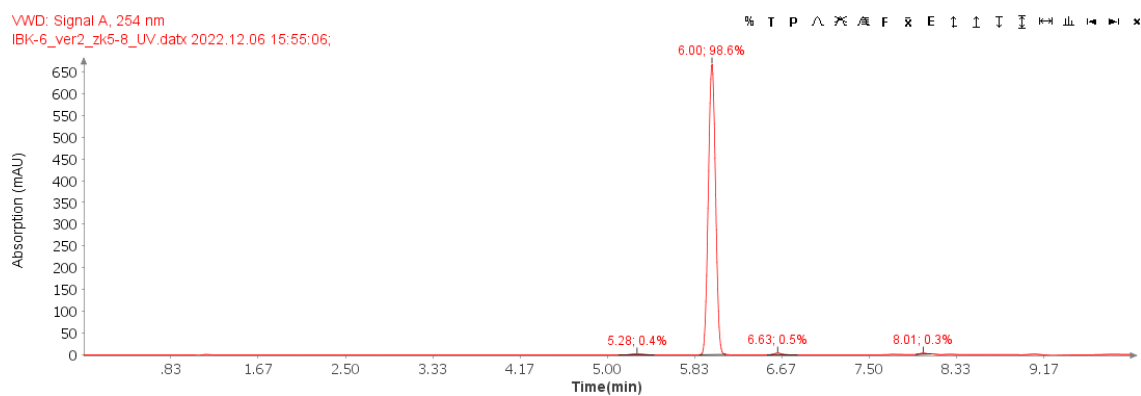
3.9 IBK-7

Name: 2-azido-1-(4-(dimethylamino)phenyl)ethan-1-one

Appearance: orange solid

Molecular weight: 204.10 g/mol
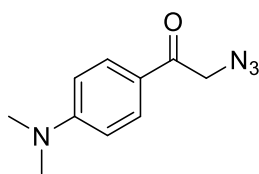
Retention factor: 0.31 (DCM)

Yield: 69 %, resp. 69 % (the reaction was repeated)

HPLC-MS (ESI+, m/z): [M+CH3CN+H]$^+$ 245.6
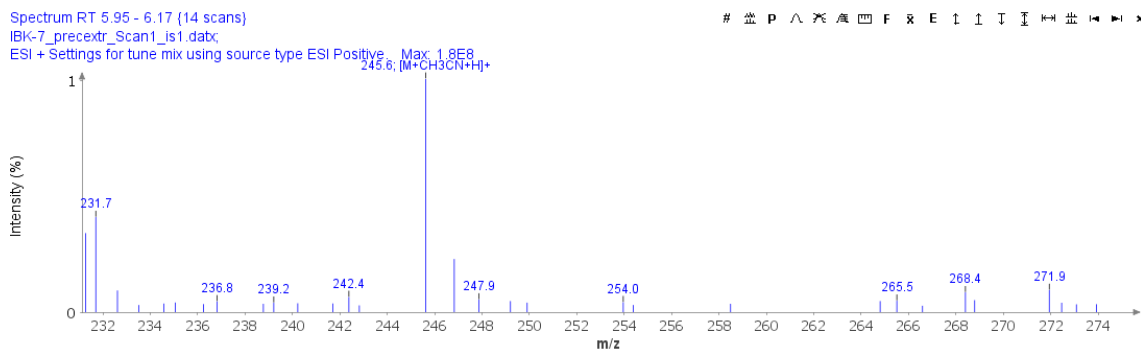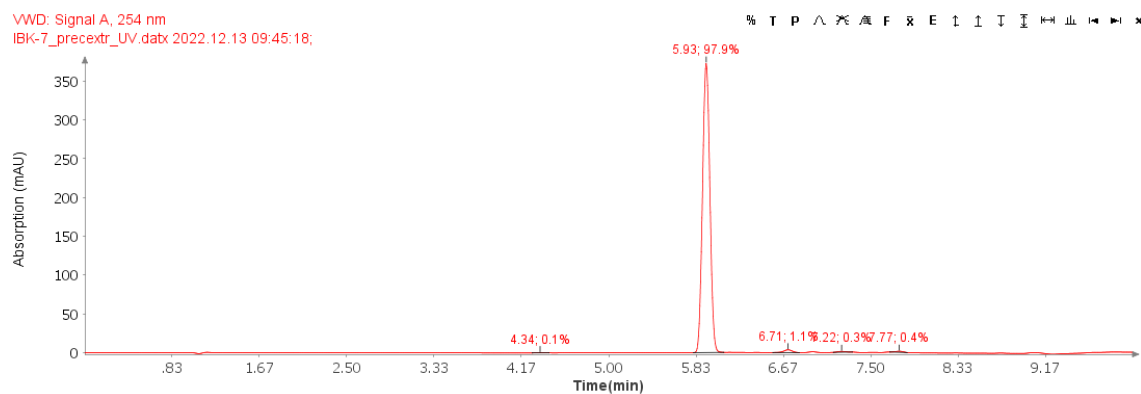
^{1}**H NMR** (400 MHz, DMSO) δ 7.82–7.73 (m, 2H), 6.78–6.70 (m, 2H), 4.71 (s, 2H), 3.03 (s, 6H)

3.10 IBK-8
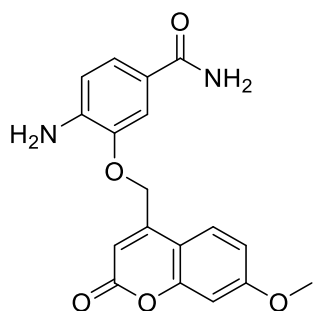
Name: 4-amino-3-((7-methoxy-2-oxo-2*H*-chromen-4-yl)methoxy)benzamide

Appearance: white solid (supposedly photosensitive)

Molecular weight: 340.11 g/mol

Retention factor: 0.39 (DCM:MeOH = 9:1)

Yield: 46 %

HPLC-MS (ESI+, m/z): [M+H]$^+$ 341.1
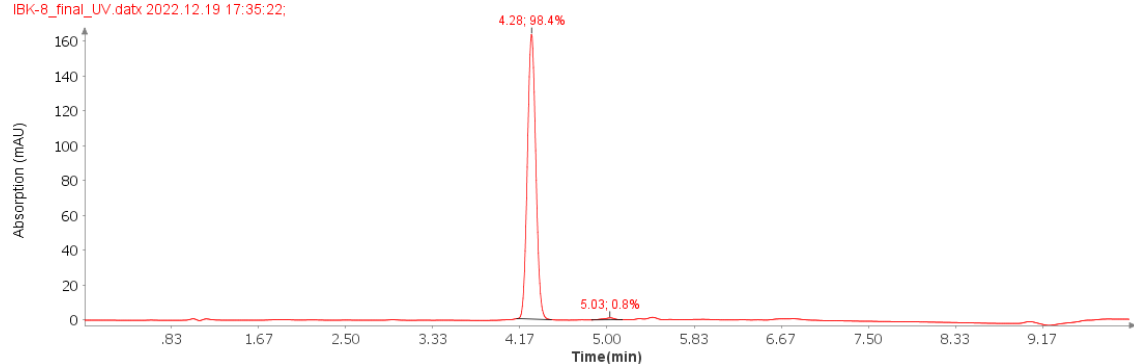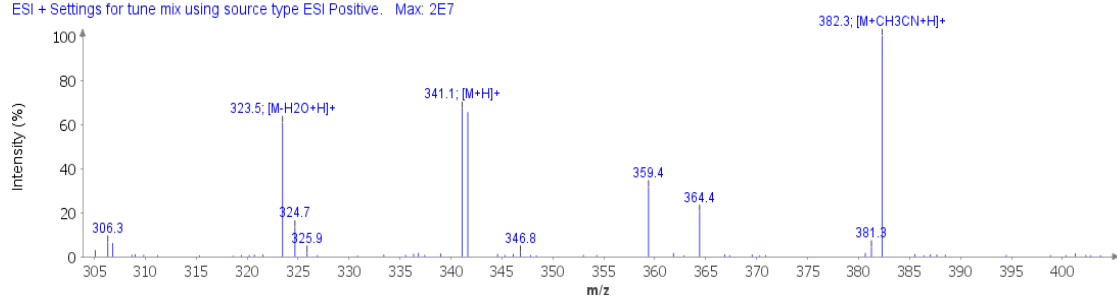
3.11 IBK-9
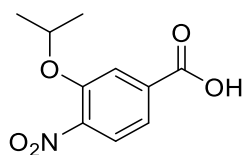
Name: 3-isopropoxy-4-nitrobenzoic acid

Appearance: sweet-smelling light brown solid

Molecular weight: 225.06 g/mol

Yield: 98 %

HPLC-MS (ESI-, m/z): [M-H]$^-$ 223.6
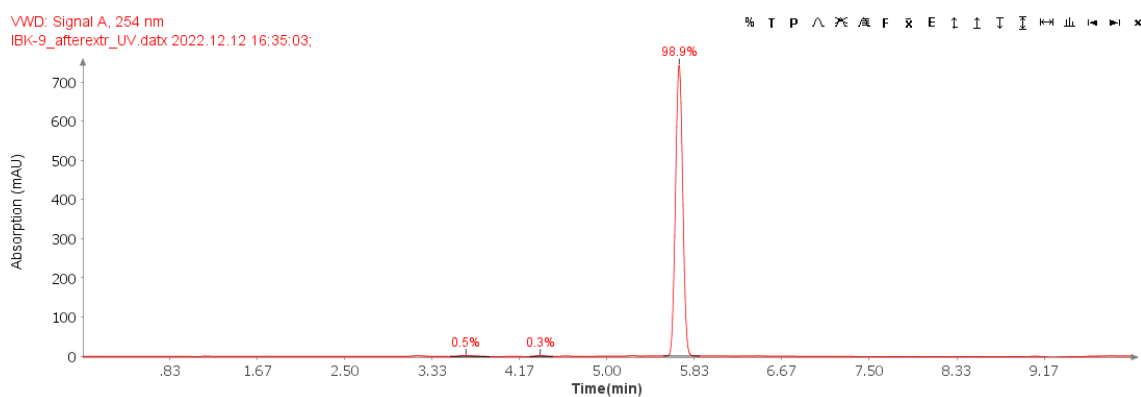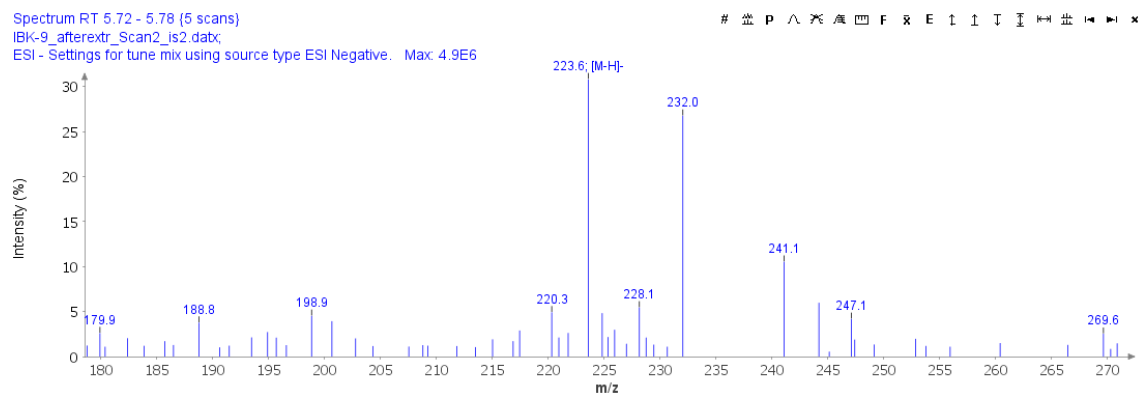
^{1}H NMR (400 MHz, DMSO) δ 13.63 (s, 1H), 7.92 (d, J = 8.3 Hz, 1H), 7.77 (d, J = 1.6 Hz, 1H), 7.62 (dd, J = 8.3, 1.6 Hz, 1H), 4.91 (hept, J = 6.0 Hz, 1H), 1.30 (d, J = 6.0 Hz, 6H)

3.12 IBK-10
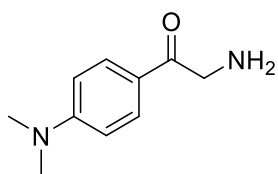
Name: 2-amino-1-(4-(dimethylamino)phenyl)ethan-1-one

Appearance: red solid

Molecular weight: 178.11 g/mol

Yield: 62 %

HPLC-MS (ESI+, m/z): [M+H]$^+$ 178.7
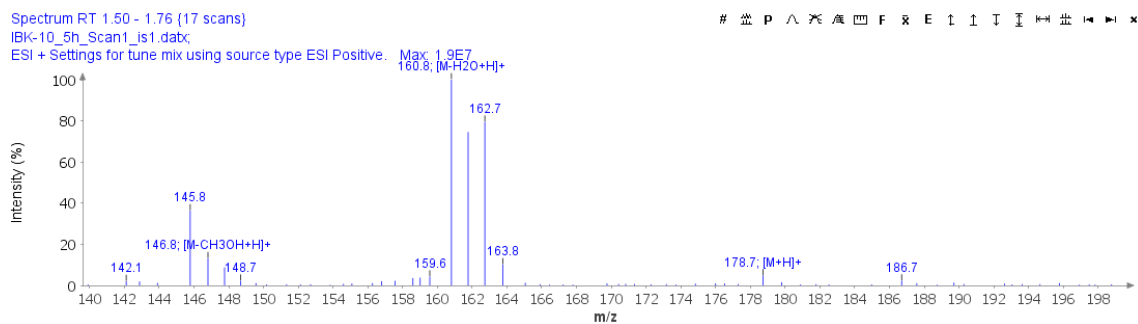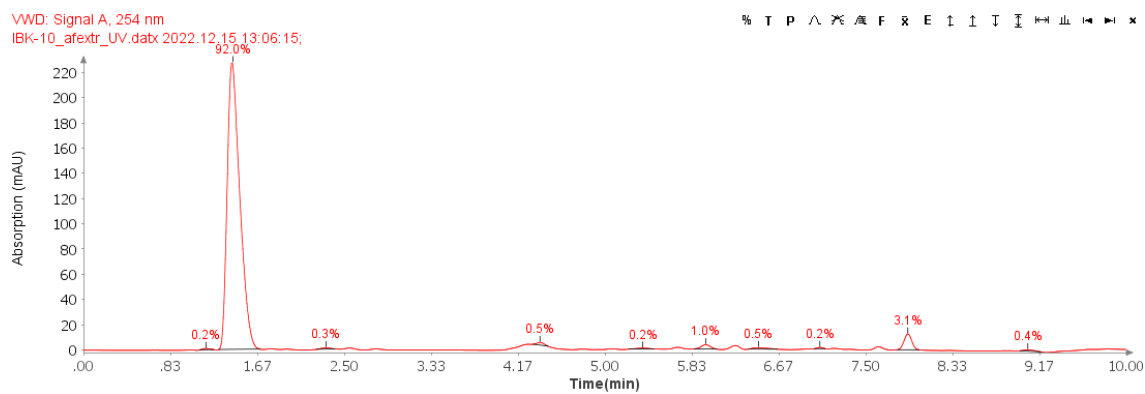
3.13 IBK-12
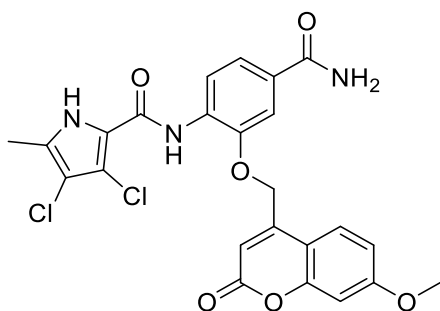
Name: *N*-(4-carbamoyl-2-((7-methoxy-2-oxo-2*H*-chromen-4-yl)methoxy)phenyl)-3,4-dichloro-5-methyl-1*H*-pyrrole-2-carboxamide

Appearance: light grey solid (supposedly photosensitive)

Molecular weight: 515.07 g/mol

Yield: 1 %

HPLC-MS (ESI+, m/z): [M+H]$^+$ 515.9
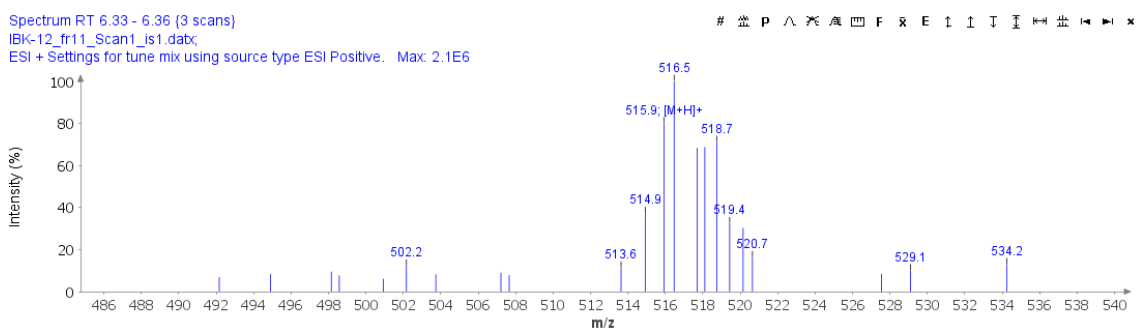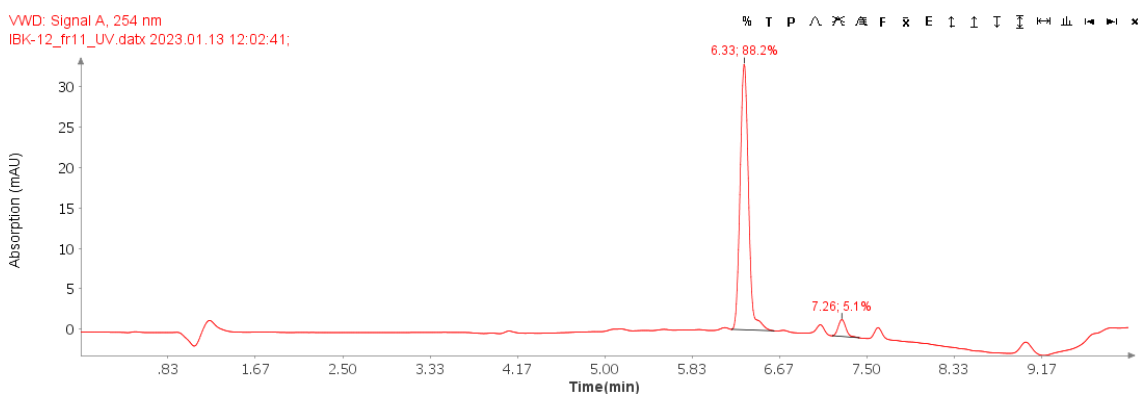
^{1}H NMR (400 MHz, DMSO) δ 12.41 (s, 1H), 9.09 (s, 1H), 8.42 (d, J = 8.4 Hz, 1H), 7.97 (s, 1H), 7.88–7.75 (m, 2H), 7.62 (dd, J = 8.4, 1.8 Hz, 1H), 7.41 (s, 1H), 7.10 (d, J = 2.4 Hz, 1H), 7.02–6.94 (m, 1H), 6.55 (s, 1H), 5.57 (d, J = 6.3 Hz, 2H), 3.87 (s, 2H), 2.21 (d, J = 2.4 Hz, 3H), 1.23 (s, 2H)

3.14 IBK-BOC
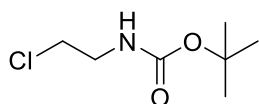
Name: *tert*-butyl (2-chloroethyl)carbamate

Appearance: yellow oily liquid with sharp smell

Molecular weight: 179.07 g/mol

Yield: 84 %

[^1]H NMR (400 MHz, DMSO) δ 7.07 (t, J = 5.7 Hz, 1H), 5.75 (s, 1H), 3.56 (t, J = 6.4 Hz, 2H), 3.23 (q, J = 6.2 Hz, 1H), 1.38 (s, 9H)

4. Methods

Analytical TLC was performed on silica gel 60 F254 aluminum sheets (0.25 mm) supplied by Merck, using visualization with UV light (254 and 366 nm) and ninhydrin.

Column chromatography was carried out on silica gel 60 with particle size 240–400 mesh.

Analytical reversed-phase HPLC/UV/MS analyses were performed on a 1260 Infinity II LC system (Agilent Technologies Inc., Santa Clara, CA, USA) using Waters XBridge C18 column (3.5 mm, 4.6 mm × 150 mm), with flow rate of 1.5 mL/min and sample injection volume of 5 µL. The mobile phase consisted of acetonitrile (solvent A) and 0.1% formic acid in 1% acetonitrile in ultrapure water (solvent B). The gradient (defined for solvent A) was: 0-1.0 min, 25%; 1.0-6.0 min, 25%-98%; 6.0-6.5 min, 98%; 6.5-7.5 min, 98%-25%; 7.5-10.5 min, 25%. HPLC was coupled with ADVION expression CMSL mass spectrometer (Advion, USA), using Capillary Temperature of 250°C and Source Gas Temperature of 200°C. For ESI source with negative polarity was used Capillary Voltage of 180V, and ESI Voltage of 2500V. For ESI source with positive polarity was used Capillary Voltage of 150V and ESI Voltage of 3500V.

^{1}H NMR spectra were recorded on a Bruker VNMR S500 (Varian, Palo Alto, CA, USA) at 400 MHz. The spectra were recorded in DMSO-d6 at ambient temperature. The chemical shifts are reported as δ values in ppm are indirectly referenced to tetramethylsilane (TMS) via the solvent signal (2.49 for ^{1}H in DMSO-d6).

This protocol for testing inhibitory activity against topo IIα was taken over from Žiga et al.[13] *Inhibitory activity against topo IIα* was determined with commercially available relaxation assay kits (Inspiralis Limited, Norwich, UK) on Pierce[TM] streptavidin coated 96-well microtiter plates (Thermo Scientific, Rockford, IL, USA). The plates were rehydrated with wash buffer (20 mM Tris·HCl, 137 mM NaCl, 0.01% w/v BSA, 0.05% v/v Tween 20, pH 7.6) and then biotinylated triplex forming oligonucleotide dissolved in wash buffer added for 5 min to immobilize. The unbound oligonucleotide was washed off with wash buffer. Next, enzymatic reaction was performed: the reaction volume of 30 µL in buffer (50 mM Tris·HCl, 10 mM MgCl2, 125 mM NaCl, 5 mM DTT, 0.1 µg/mL albumin, 1 mM ATP, pH 7.5) contained 0.75 µg of supercoiled pNO1 plasmid, 1.5 U of human DNA topoisomerase II, inhibitor, 1% DMSO and 0.008% Tween 20. Reaction mixtures were incubated at 37 °C for 30 min. After that, the TF buffer (50 mM NaOAc, 50 mM NaCl and 50 mM MgCl2, pH 5.0) was added and the mixtures were left for 30 min

at RT, during which biotin–oligonucleotide–plasmid triplex was formed. The unbound plasmid was washed off with TF buffer. Then the solution of Diamond Dye in T10 buffer (10 mM Tris·HCl, 1 mm EDTA, pH 8.0) was added. After 15 min of incubation in the dark, fluorescence was measured with a microplate reader (BioTek Synergy H4, excitation: 485 nm, emission: 537 nm). Initial screening was done at 10 and 100 µM concentrations of inhibitors. As the positive control, etoposide (TCI, Tokyo, Japan; $IC_{50} = 71$ µM) was used.

5. Conclusions

The synthesis of IBK-12 was achieved through a multi-step procedure. Starting from esterification of 3-hydroxy-4-nitrobenzioc acid (Scheme 1, a) resulting in methyl ester (IBK-1; yield 98 %), followed by ammonolysis of the obtained methyl ester (Scheme 1, b). Yielded amide (IBK-2; yield 71 %) was later purified using extraction between 5% $NaHCO_3$ water solution and ethyl acetate to remove the starting 3-hydroxy-4-nitrobenzioc acid as an impurity. High purity of IBK-2 appeared to be important for the following reaction. This reaction (Scheme 1, c) was repeated three times, each time with optimized reaction conditions, to obtain the desired product. Considering optimizations in reaction conditions, following details are suggested to be important for successful preparation of IBK-3 – high purity of the starting IBK-2, argon atmosphere to avoid air moisture, KI as an *in situ* catalyst and stirring the reaction mixture at room temperature protected from light. After optimizations, IBK-3 was obtained with a high yield (96 %) and purity, therefore it was used for the next step without further purification. Next step was reduction of the nitro group (Scheme 1, d). The product (IBK-8) was obtained after extraction to ethyl acetate with yield 46 %. The last step was coupling of IBK-8 from the previous reaction with 3,4-dichloro-5-methyl-1*H*-pyrrole-2-carboxylic acid (Scheme 1, e). First, the acid was activated using thionyl chloride under argon atmosphere to prevent the formed acyl chloride from decomposing by air moisture. After the coupling, final compound IBK-12 was purified to allow *in vitro* testing. Two main impurities (one of them being the starting 3,4-dichloro-5-methyl-1*H*-pyrrole-2-carboxylic acid) and one minor impurity were detected in the reaction mixture. The starting acid was removed by suspending the crude in DCM – the acid dissolved, and precipitate was filtered off. One major impurity and one minor impurity remained in the crude. Therefore, further purification had to be done. Column chromatography was performed twice to obtain a very small amount of the final product (3 mg of IBK-12). Purification process was complicated due to poor solubility of the final product and impurities. Optimization of the acylation step (Scheme 1, e) would be beneficial to obtain purer product with better yield. It might be favorable to perform the reaction at lower temperature than chosen 115°C and in different solvent considering previous experience with reaction intermediates (IBK-3, IBK-8).

IBK-12 was tested for its inhibitory activity on human topoisomerase IIα using commercially available relaxation assay kits (Inspiralis Limited, Norwich, UK)

with result $IC_{50} > 200$ µM (no on-target activity). Further testing of IBK-12 will be needed in future to determine fluorophore properties of the compound, such as absorption maximum and emission maximum wavelengths. Also, solubility and metabolic stability of the compound will be determined. Furthermore, IBK-12 could be used for cell analysis using a fluorescence cell microscopy to observe the distribution of the compound and interactions with various components of the cell. Unfortunately, since the yield of IBK-12 after purification was low (1 %; 3 mg), the synthesis will most likely have to be repeated to perform the intended evaluations.

The aim was to prepare two more compounds and test them for their inhibitory activity on human topoisomerase IIα, however the synthesis of these compounds was not successful (Scheme 9 and Scheme 17). Preparation of IBK-11 (Scheme 9) failed in the last step of the synthetic procedure. A main impurity was isolated from the reaction mixture, but identification of the impurity was not accomplished due to insolubility of the compound. Synthesis of IBK-5 (Scheme 17) was not successful despite many attempts to optimize reaction conditions.

In total, eleven compounds were prepared during the project. One on them being final compound (not previously described in literature – SciFinder, accessed 11.05.2023) later submitted for further *in vitro* testing and ten of them being reaction intermediates.

6. Literature

1. Skok, Ž., Durcik, M., Zajec, Ž., Gramec Skledar, D., Bozovičar, K., Pišlar, A., Tomašič, T., Zega, A., Peterlin Mašič, L., Kikelj, D., Zidar, N., & Ilaš, J. (2023). ATP-competitive inhibitors of human DNA topoisomerase IIα with improved antiproliferative activity based on N-phenylpyrrolamide scaffold. *European journal of medicinal chemistry*, *249*, 115116. https://doi.org/10.1016/j.ejmech.2023.115116

2. https://gco.iarc.fr/today/online-analysis-tablerc.fr (accessed: 11.05.2023)

3. https://www.cancer.gov/about-cancer/treatment/side-effects (accessed: 11.05.2023)

4. Ioele, G., Chieffallo, M., Occhiuzzi, M. A., De Luca, M., Garofalo, A., Ragno, G., & Grande, F. (2022). Anticancer Drugs: Recent Strategies to Improve Stability Profile, Pharmacokinetic and Pharmacodynamic Properties. *Molecules (Basel, Switzerland)*, *27*(17), 5436. https://doi.org/10.3390/molecules27175436

5. Champoux J. J. (2001). DNA topoisomerases: structure, function, and mechanism. *Annual review of biochemistry*, *70*, 369–413. https://doi.org/10.1146/annurev.biochem.70.1.369

6. Deweese, J. E., Osheroff, M. A., & Osheroff, N. (2009). DNA topology and topoisomerases. *Biochemistry and Molecular Biology Education*, *37*(1), 2–10. https://doi.org/10.1002/bmb.20244

7. McClendon, A. K., & Osheroff, N. (2007). DNA topoisomerase II, genotoxicity, and cancer. *Mutation research*, *623*(1-2), 83–97. https://doi.org/10.1016/j.mrfmmm.2007.06.009

8. Vann, K. R., Oviatt, A. A., & Osheroff, N. (2021). Topoisomerase II Poisons: Converting Essential Enzymes into Molecular Scissors. *Biochemistry*, *60*(21), 1630–1641. https://doi.org/10.1021/acs.biochem.1c00240

9. Delgado, J. L., Hsieh, C. M., Chan, N. L., & Hiasa, H. (2018). Topoisomerases as anticancer targets. *The Biochemical journal, 475*(2), 373–398. https://doi.org/10.1042/BCJ20160583

10. Soren, B. C., Dasari, J. B., Ottaviani, A., Iacovelli, F., & Fiorani, P. (2020). Topoisomerase IB: a relaxing enzyme for stressed DNA. *Cancer drug resistance (Alhambra, Calif.)*, *3*(1), 18–25. https://doi.org/10.20517/cdr.2019.106

11. Krogh, B. O., & Shuman, S. (2002). A poxvirus-like type IB topoisomerase family in bacteria. *Proceedings of the National Academy of Sciences of the United States of America*, *99*(4), 1853–1858. https://doi.org/10.1073/pnas.032613199

12. Larsen, A. K., Escargueil, A. E., & Skladanowski, A. (2003). Catalytic topoisomerase II inhibitors in cancer therapy. *Pharmacology & therapeutics*, *99*(2), 167–181. https://doi.org/10.1016/s0163-7258(03)00058-5

13. Skok, Ž., Durcik, M., Gramec Skledar, D., Barančoková, M., Peterlin Mašič, L., Tomašič, T., Zega, A., Kikelj, D., Zidar, N., & Ilaš, J. (2020). Discovery of new ATP-competitive inhibitors of human DNA topoisomerase IIα through screening

of bacterial topoisomerase inhibitors. *Bioorganic chemistry*, *102*, 104049. https://doi.org/10.1016/j.bioorg.2020.104049

14. Bollimpelli, V. S., Dholaniya, P. S., & Kondapi, A. K. (2017). Topoisomerase IIβ and its role in different biological contexts. *Archives of biochemistry and biophysics*, *633*, 78–84. https://doi.org/10.1016/j.abb.2017.06.021

15. Pendleton, M., Lindsey, R. H., Jr, Felix, C. A., Grimwade, D., & Osheroff, N. (2014). Topoisomerase II and leukemia. *Annals of the New York Academy of Sciences*, *1310*(1), 98–110. https://doi.org/10.1111/nyas.12358

16. Botella, P., & Rivero-Buceta, E. (2017). Safe approaches for camptothecin delivery: Structural analogues and nanomedicines. *Journal of controlled release : official journal of the Controlled Release Society*, *247*, 28–54. https://doi.org/10.1016/j.jconrel.2016.12.023

17. Martino, E., Della Volpe, S., Terribile, E., Benetti, E., Sakaj, M., Centamore, A., Sala, A., & Collina, S. (2017). The long story of camptothecin: From traditional medicine to drugs. *Bioorganic & medicinal chemistry letters*, *27*(4), 701–707. https://doi.org/10.1016/j.bmcl.2016.12.085

18. https://drugcentral.org/drugcard/296?q=belotecancentral.org (accessed: 10.05.2023)

19. Khaiwa, N., Maarouf, N. R., Darwish, M. H., Alhamad, D. W. M., Sebastian, A., Hamad, M., Omar, H. A., Orive, G., & Al-Tel, T. H. (2021). Camptothecin's journey from discovery to WHO Essential Medicine: Fifty years of promise. *European journal of medicinal chemistry*, *223*, 113639. https://doi.org/10.1016/j.ejmech.2021.113639

20. Narayan, P., Osgood, C. L., Singh, H., Chiu, H. J., Ricks, T. K., Chiu Yuen Chow, E., Qiu, J., Song, P., Yu, J., Namuswe, F., Guiterrez-Lugo, M., Hou, S., Pierce, W. F., Goldberg, K. B., Tang, S., Amiri-Kordestani, L., Theoret, M. R., Pazdur, R., & Beaver, J. A. (2021). FDA Approval Summary: Fam-Trastuzumab Deruxtecan-Nxki for the Treatment of Unresectable or Metastatic HER2-Positive Breast Cancer. *Clinical cancer research : an official journal of the American Association for Cancer Research*, *27*(16), 4478–4485. https://doi.org/10.1158/1078-0432.CCR-20-4557

21. Andrikopoulou, A., Zografos, E., Liontos, M., Koutsoukos, K., Dimopoulos, M. A., & Zagouri, F. (2021). Trastuzumab Deruxtecan (DS-8201a): The Latest Research and Advances in Breast Cancer. *Clinical breast cancer*, *21*(3), e212–e219. https://doi.org/10.1016/j.clbc.2020.08.006

22. Drwal, M. N., Marinello, J., Manzo, S. G., Wakelin, L. P., Capranico, G., & Griffith, R. (2014). Novel DNA topoisomerase IIα inhibitors from combined ligand- and structure-based virtual screening. *PloS one*, *9*(12), e114904. https://doi.org/10.1371/journal.pone.0114904

23. Skok, Ž., Zidar, N., Kikelj, D., & Ilaš, J. (2020). Dual Inhibitors of Human DNA Topoisomerase II and Other Cancer-Related Targets. *Journal of medicinal chemistry*, *63*(3), 884–904. https://doi.org/10.1021/acs.jmedchem.9b00726

24. Cowell, I. G., & Austin, C. A. (2012). Mechanism of generation of therapy related leukemia in response to anti-topoisomerase II agents. *International journal of environmental research and public health*, *9*(6), 2075–2091. https://doi.org/10.3390/ijerph9062075

25. Lyu, Y. L., Kerrigan, J. E., Lin, C. P., Azarova, A. M., Tsai, Y. C., Ban, Y., & Liu, L. F. (2007). Topoisomerase IIbeta mediated DNA double-strand breaks: implications in doxorubicin cardiotoxicity and prevention by dexrazoxane. *Cancer research*, *67*(18), 8839–8846. https://doi.org/10.1158/0008-5472.CAN-07-1649

26. Jirkovský, E., Jirkovská, A., Bavlovič-Piskáčková, H., Skalická, V., Pokorná, Z., Karabanovich, G., Kollárová-Brázdová, P., Kubeš, J., Lenčová-Popelová, O., Mazurová, Y., Adamcová, M., Lyon, A. R., Roh, J., Šimůnek, T., Štěrbová-Kovaříková, P., & Štěrba, M. (2021). Clinically Translatable Prevention of Anthracycline Cardiotoxicity by Dexrazoxane Is Mediated by Topoisomerase II Beta and Not Metal Chelation. *Circulation. Heart failure*, *14*(11), e008209. https://doi.org/10.1161/CIRCHEARTFAILURE.120.008209

27. Chène, P., Rudloff, J., Schoepfer, J., Furet, P., Meier, P., Qian, Z., Schlaeppi, J. M., Schmitz, R., & Radimerski, T. (2009). Catalytic inhibition of topoisomerase II by a novel rationally designed ATP-competitive purine analogue. *BMC chemical biology*, *9*, 1. https://doi.org/10.1186/1472-6769-9-1

28. Bailly C. (2012). Contemporary challenges in the design of topoisomerase II inhibitors for cancer chemotherapy. *Chemical reviews*, *112*(7), 3611–3640. https://doi.org/10.1021/cr200325f

29. Kabir, M. L., Wang, F., & Clayton, A. H. A. (2022). Intrinsically Fluorescent Anti-Cancer Drugs. *Biology*, *11*(8), 1135. https://doi.org/10.3390/biology11081135

30. Sun, X. Y., Liu, T., Sun, J., & Wang, X. J. (2020). Synthesis and application of coumarin fluorescence probes. *RSC advances*, *10*(18), 10826–10847. https://doi.org/10.1039/c9ra10290f

31. Carneiro, A., Matos, M. J., Uriarte, E., & Santana, L. (2021). Trending Topics on Coumarin and Its Derivatives in 2020. *Molecules (Basel, Switzerland)*, *26*(2), 501. https://doi.org/10.3390/molecules26020501

32. Cao, D., Liu, Z., Verwilst, P., Koo, S., Jangjili, P., Kim, J. S., & Lin, W. (2019). Coumarin-Based Small-Molecule Fluorescent Chemosensors. *Chemical reviews*, *119*(18), 10403–10519. https://doi.org/10.1021/acs.chemrev.9b00145

33. Wu, C., Wang, J., Shen, J., Bi, C., & Zhou, H. (2017). Coumarin-based Hg2+ fluorescent probe: Synthesis and turn-on fluorescence detection in neat aqueous solution. *Sensors and Actuators, B: Chemical*, *243*, 678–683. https://doi.org/10.1016/j.snb.2016.12.046

34. Zhang, X. F., Zhang, T., Shen, S. L., Miao, J. Y., & Zhao, B. X. (2015). A ratiometric lysosomal pH probe based on the coumarin-rhodamine FRET system. *RSC Advances*, *5*(61), 49115–49121. https://doi.org/10.1039/c5ra06246b

35. Antina, E., Bumagina, N., Marfin, Y., Guseva, G., Nikitina, L., Sbytov, D., & Telegin, F. (2022). BODIPY Conjugates as Functional Compounds for Medical Diagnostics and Treatment. *Molecules (Basel, Switzerland)*, *27*(4), 1396. https://doi.org/10.3390/molecules27041396

36. Zidar, N., Montalvão, S., Hodnik, Ž., Nawrot, D. A., Žula, A., Ilaš, J., Kikelj, D., Tammela, P., & Mašič, L. P. (2014). Antimicrobial activity of the marine alkaloids, clathrodin and oroidin, and their synthetic analogues. *Marine drugs*, *12*(2), 940–963. https://doi.org/10.3390/md12020940

37. Lu, J., Patel, S., Sharma, N., Soisson, S. M., Kishii, R., Takei, M., Fukuda, Y., Lumb, K. J., & Singh, S. B. (2014). Structures of kibdelomycin bound to Staphylococcus aureus GyrB and ParE showed a novel U-shaped binding mode. *ACS chemical biology, 9*(9), 2023–2031. https://doi.org/10.1021/cb5001197

38. Diwu, Z., Beachdel, C., & Klaubert, D. H. (1998). A facile protocol for the convenient preparation of amino-substituted α-bromo- and α,α-dibromo arylmethylketones. *Tetrahedron Letters*, *39*(28), 4987–4990. https://doi.org/10.1016/S0040-4039(98)00975-7

39. https://www.webelements.com/bromine/isotopes.html (accessed: 13.05.2023)